

Response to reviewers' comments

We thank the reviewers for their thoughtful comments. We have carefully revised the manuscript accordingly. Our point-to-point responses to the reviewers' comments, which are repeated in italic, are given below.

ACPD manuscript: **10.5194/acpd-14-21149-2014**

Authors: **L. Yu, J. Smith, A. Laskin, C. Anastasio, J. Laskin, and Q. Zhang**

Reviewer #1

Yu et al studied the formation of non-volatile organic compounds through two aqueous mechanisms: oxidation via OH radical initiated by HOOH photolysis, and oxidation through $^3C^$ initiated by photolysis of an aromatic aldehyde (which also includes OH oxidation due to the formation of HOOH via this route). The authors used a variety of analytical methods to describe the composition of the SOA at the half-way reaction mark. This study builds upon Sun et al (2010), adding a molecular-composition analysis based on both positive and negative ion mode high-resolution nano-DESI MS. The authors conclude that hydroxylation and various oligomerization reactions (e.g., coupling of phenoxy and aromatic alkyl radicals) are responsible for the aqueous SOA formation. This is an interesting analytical study that offers insight into a class of poorly-understood reaction mechanism in the aqueous phase, and should be published as such. There are areas that would benefit from clarification and further discussion, which I outline in the specific comments. In particular, it would be valuable to discuss mechanistic differences in guaiacol, syringol, and phenol in terms of the additional methoxy groups as activating substituents in the OH/ $^3C^*$ or abstraction vs. addition pathways of these radicals.*

Authors' reply #1: We have added some discussions on the influence of additional methoxy group on the reactivity of phenols in Sect. 3.1: "The reactivity differences among the three precursors are likely due to the electron-donating effect of the o-methoxy substituents, which may significantly increase the rate of electrophilic reactions on the benzene ring."

Reviewer's comment:

1. Including structures of guaiacol, syringol, and phenol would be helpful for understanding the discussion in the introduction and much of the text.

Authors' reply #2: As suggested, we added the structures of syringol, guaiacol, and phenol in Table 1.

Reviewer's comment:

2. The authors state in several areas a consistency with Smith et al that the aromatic species react "faster" with $^3C^$ than OH. What does this mean exactly? Are the reaction rate coefficients $k_{^3C^*} > k_{OH}$ or the effective rates $k_{^3C^*}[^3C^*] > k_{OH}[OH]$? If the former, what is the ratio? If the latter, can the authors make such a meaningful comparison without knowing $[^3C^*]$ that is*

derived from 5uM 3,4DMB+hv and [OH] from 100uM HOOH +hv? Further, as the $^3C^$ study includes OH oxidation (Fig 7), how can the entirety of the reaction be attributed to $^3C^*$?*

Authors' reply #3: Our statement of phenols reacting faster with $^3C^*$ than with $\bullet OH$ is based on the effective, or pseudo first-order rate constants for phenol loss (k'_{ArOH}) measured in our experiments, i.e., $k_3C^*[^3C^*] > k_{OH}[OH]$. Since the pseudo first-order rate is the product of the bimolecular rate constant and the steady state concentration of the oxidant: $k'_{ArOH} = k_{ArOH+Oxidant}[Oxidant]$, it is true that k'_{ArOH} is dependent on oxidant concentrations. However, since the steady state concentrations of $\bullet OH$ and $^3C^*$ in our reaction systems are comparable to the concentrations of these oxidants in atmospheric drops, the comparison of k'_{ArOH} is meaningful. Based on the average k'_{ArOH} values from our syringol experiments ($2.5 \times 10^{-4} s^{-1}$ for syringol + $^3C^*$ and $1.0 \times 10^{-4} s^{-1}$ for syringol + $\bullet OH$), and the bimolecular rate constants determined by Smith et al. (in preparation for PCCP), we calculate that steady state concentrations of $^3C^*$ and $\bullet OH$ during our experiments are $6.9 \times 10^{-14} mol L^{-1}$ and $5.1 \times 10^{-15} mol L^{-1}$, respectively. Thus, the $\bullet OH$ steady state concentration in our solution is similar to the aqueous $[OH]$ measured in fog and cloud waters (Anastasio and McGregor, 2001; Arakaki et al., 2013). Although there are no reported literature values for $[^3C^*]$ in ambient fog/cloud waters, recent, not-yet published results from Anastasio's group suggest a similar order of magnitude of $[^3C^*]$ in Davis fog water. These points are now clarified in Sect. 3.1.

In terms of the question of whether the phenol loss in reactions with $^3C^*$ can be entirely attributed to $^3C^*$, we believe the $\bullet OH$ contribution was minor. While Anastasio et al. (1997) showed that HOOH, a precursor for $\bullet OH$, is produced from reactions of phenols with $^3C^*$, the amount of HOOH produced is small and $\bullet OH$ oxidation in the triplet experiments appears to be negligible (Smith et al., 2014). Approximately 4-7 molecules of phenol are destroyed for every molecule of HOOH produced under the experimental conditions similar to those used in this study, suggesting that a majority of the photodestroyed phenol leads to products other than HOOH. In response to the reviewer's comments, we now added the sentence in Sect 3.2: "Note that the amount of HOOH produced in the reactions of phenols + $^3C^*$ is small and $\bullet OH$ oxidation appears to be negligible compared to $^3C^*$ oxidation (Smith et al., 2014)."

Reviewer's comment:

3. Additional to the above comment, can the authors provide estimates of steady-state [Oxidant] from HPLC-UV decay trace of the aromatic precursors?

Authors' reply #4: The steady state concentrations of $\bullet OH$ and $^3C^*$ during this study are estimated at $5.1 \times 10^{-15} mol L^{-1}$ and $6.9 \times 10^{-14} mol L^{-1}$, respectively, for syringol, $1.4 \times 10^{-15} mol L^{-1}$ and $2.6 \times 10^{-14} mol L^{-1}$, respectively, for guaiacol, $4.4 \times 10^{-16} mol L^{-1}$ and $7.4 \times 10^{-14} mol L^{-1}$, respectively, for phenol. This information is now provided in Sect. 3.1.

Reviewer's comment:

4. [Experimental methods] The authors explain later in the text that the reason they blow dry one sample (then later reconstitute in water) and freeze dry the other is to remove the semivolatiles from the blow dry case. Why not explicitly state this in the experimental methods?

Authors' reply #5: Done as suggested. By the way, we did not freeze dry samples. The flash-frozen samples were prepared by rapidly freezing the solutions using liquid nitrogen. These

samples were stored in the dark under -20 °C and were thawed inside a refrigerator (~ 4°C) prior to analysis. The procedures for AMS analysis of the thawed flash-frozen sample and the reconstituted blown-down samples are exactly the same.

Reviewer's comment:

5. [Experimental methods] If Milli-Q water served as the analytical blank, did the mass of 3,4DMB count towards the mass yield of the ³C* oxidation system? Were controls performed in the photolysis of 3,4DMB alone and evaporated in the same way?

Authors' reply #6: The mass of 3,4-DMB was removed from the calculation of the aqSOA mass yields. Control experiments were performed to examine the photolysis of 3,4-DMB alone and the resulting solutions were evaporated in the same way as treating the aqSOA samples. No formation of aqSOA was observed. The results of the control experiments are shown in Smith et al. (2014) (Figure S8 in the Supporting Information). In response to reviewer's comments, we added the sentence: "In addition, no formation of aqSOA was observed in control experiments in which 3,4-DMB was illuminated alone under the same condition and the resulting solution evaporated in the same way." at the end of Sect. 2.1.

Reviewer's comment:

6. [21158, line 1] What is the significance of "near 100%" mass yield, when this value can be exceeded from oxygen incorporation into the phenolic structure?

Authors' reply #7: Assuming no carbon losses, i.e., no formation of volatile and semivolatile species that evaporate during the experiments or the drying processes, the mass yields of phenol, guaiacol, and syringol should be 201%, 161%, and 143%, respectively, for ³C*-mediated reactions, and 214%, 184% and 142%, respectively, for •OH-mediated reactions, based on comparing the OM/OC ratios of the aqSOA and the corresponding precursors. We added this information in Sect. 3.1: "Based on comparing to the OM/OC of the precursors, the mass yields of the aqSOA should be 142-214% assuming all reacted phenols were converted into low volatility species. However, the measured values are 16-38% lower, indicating that approximately 16-38% of the reacted phenols were converted into volatile and semi-volatile species that evaporated during illumination and/or drying."

Reviewer's comment:

7. [21158, lines 26-29] I find this speculation strange. Why would ESI efficiency (in both pos/neg mode) be reduced for "highly oxidized species" when the positive mode ionization is partially cluster formation and the negative mode ionization is deprotonation? Also, more support is needed if one is to claim that ESI alone causes decarboxylation of organic acids – as this ionization mechanism should be excellent for the detection of organic acids in the negative mode without extensive fragmentation. Do authors have evidence that certain carboxylic acids standards undergo this instrument-assisted decomposition in standard ESI? Levsen et al 2007 that is cited is not appropriate here, as Levsen and coauthors studied losses of neutrals from precursor ions through collision-induced dissociation in an ion trap (e.g., energy was supplied to purposefully fragment ions) as opposed to this study.

Authors' reply #8: We agree with the reviewer's comments, and removed related discussions in the revised manuscript.

Reviewer's comment:

8. [21159, lines 1-5] *After considering the 1 – 4% of organic acids that were not analyzed in nano-DESI, what would the corrected O/C be? My assumption is that it does not make much of a difference in the O/C.*

Authors' reply #9: By considering 1-4% of organic acids that were not analyzed in nano-DESI the O/C would increase by 0.03-0.05. The sentence now reads: "According to IC analysis, these small organic anions together represent 0.8-3.8% of the TOC of aqSOA (Table 1). Therefore accounting them for these species would only increase the nano-DESI O/C values by 0.03-0.05".

Reviewer's comment:

9. [21160, lines 6-7] *Specifically which kind of functional groups in phenol aqSOA would not be well-ionized by both the positive and negative mode nano-DESI that was used here? If there is an aromatic group intact, (+) nano-DESI should ionize these compounds well.*

Authors' reply #10: In negative ion mode nano-DESI analysis, phenol and carboxyl groups should be readily ionized while aldehyde, ketone, and methoxy groups are ionized less efficiently. In positive ion mode nano-DESI analysis, larger oligomers containing multiple carbonyl groups form sodium adducts. All other groups in phenolic compounds are not very well ionized in positive ion mode.

Reviewer's comment:

10. [21164, line 3] *The AMS results are only quantitative if the specific ion (e.g., C₁₆H₁₈O₆⁺) does not show up as smaller fragments, thus dispersing the signal of the molecule. Do authors have evidence that this is the case from calibrations with standards? Further, this is nitrate-equivalent mass which has its own assumptions about ionization and line-transfer efficiency.*

Authors' reply #11: Since the fragment pattern of 70 eV EI mass spectrometry is reproducible (McLafferty and Turecek, 1993), unique ions can be used as tracer species to quantify the concentration of the parent compound. We will examine the quantification of individual compounds using AMS in details in future studies. We added the sentences "Since the fragmentation pattern from 70 eV electron ionization is reproducible (McLafferty and Turecek, 1993), unique ions can be used as tracer species to quantify the concentration of the parent compound." in Sect. 3.3.

Reviewer's comment:

11. [21165, lines 1-4] *Can the authors expand on why the structures of guaiacol and syringol would lead to these observed mechanistic differences?*

Authors' reply #12: It is unclear to us why guaiacol aqSOA are composed of more oligomers and derivatives than syringol aqSOA are. One possible reason is that guaiacol oligomers are more stable than syringol oligomers. This is a topic that will be subjected to future research.

Reviewer's comment:

12. [21166, lines 5-6] *The authors mention that they examined the optical properties of “phenolic aqSOA” but only discuss syringol? Do phenol and guaiacol follow the same general behavior? Why not show their spectra?*

Authors' reply #13: The aqSOA of phenol and guaiacol also show enhanced absorption in the UV-Vis region. The optical properties of phenolic aqSOA will be reported in detail in a publication in the near future (Smith et al., in preparation). We added the sentence in Sect. 3.4: “Phenol and guaiacol aqSOA also show enhanced absorption in the tropospheric sunlight wavelengths (> 300 nm), while phenol and guaiacol themselves do not.”

Reviewer's comment:

13. [21166, line 18] *Again, this is an interesting point, i.e., that the $t_{1/2}$ reactivities is higher for compounds with fewer methoxy groups within one oxidation system, that should be expanded to discuss structure-activity relationships.*

Authors' reply #14: Precursors with fewer methoxy groups react more slowly with the oxidant, and have longer half-lives under illumination. We attribute the positive correlation between the reactivities and methoxy groups to the electron-donating effect of the o-methoxy substituents, which can increase the rate of electrophilic reactions on the benzene ring by large factors. We mentioned this point in Sect. 3.1

Reviewer's comment:

14. [21167, lines 15-end] *While the particular AMS ions listed appear to be useful in this single-precursor system study, I disagree that these nominal mass assignments can be “signatures” in the ambient environment. Concerns about EI fragmentation aside, nominal mass resolution at a high m/z as 306 produces a large array of possible molecular formula candidates when sources are unknown. In the atmosphere, there is little evidence that these molecular formulas are unique to a particular chemical system. The authors should also consider the possibility that nominal even-mass ions like 306 can be assigned to either a $C_xH_yO_z$ aromatic ion radical or $C_xH_yO_zN$ cation in the atmosphere. For identifying the impact of phenolic aqSOA, it seems more promising to apply nano-DESI, as the authors have done, to field samples than AMS.*

Authors' reply #15: We agree that it is interesting to apply nano-DESI to field samples in order to identify phenolic aqSOA in ambient air and we indeed plan to do so in the future. But it is challenging to use nano-DESI for quantification, although progress has been made in this aspect (Nguyen et al., 2013). On the other hand, AMS uses 70 eV electron impact ionization, and the EI fragmentation pattern is reproducible, which allows for the identification and quantification of individual molecule in the mixture (McLafferty and Turecek, 1993). The EI ionization may also generate unique ions that are representative of the parent molecules. It is therefore viable to apply AMS signature ions for identifying phenolic aqSOA species and analyzing. We have revised this paragraph to make these points clearer. It now reads: “Overall, our results indicate that aqueous-phase processing of phenols represents an important pathway for the production of low-volatility, highly oxygenated and high molecular weight species, which remain in the particle phase after water evaporation. Since phenolic aqSOA are both water soluble and light

absorbing, understanding the impacts of these reactions on the chemical and physical properties, and thus the climatic and health effects, of atmospheric particles may be important, especially in regions influenced by biomass burning emissions. An approach for evaluating the importance of phenolic aqSOA formation in the atmosphere is to systematically analyze the AMS mass spectra of ambient aerosol for signature ions representative of phenolic aqSOA. AMS has been broadly applied for chemical analysis of ambient aerosol and multivariate statistical approaches (e.g., positive matrix factorization) have been frequently used on organic aerosol mass spectral data to determine factors representing different sources and processes (Ulbrich et al., 2009; Zhang et al., 2011). An important criterion for validating the extracted factor is via examining the mass spectra of the factors for signature ions (Zhang et al., 2011). The fact that AMS uses 70 eV EI ionization, which ionizes and fragments molecules with reproducible pattern (McLafferty and Turecek, 1993), allows for the identification and quantification of certain compounds or compound classes in a mixture via signature ions. Indeed, previous studies have demonstrated the capability of using unique AMS ions to fingerprint species such as hydrocarbon-like and oxygenated organic aerosols (Zhang et al., 2005), polycyclic aromatic hydrocarbons (PAH) (Dzepina et al., 2007), methanesulfonic acid (MSA) (Ge et al., 2012), and certain nitrogen- and sulfur-containing organic aerosols (Farmer et al., 2010; Ge et al., 2014).

With this in mind, in this study, we identified several ions that are potentially representative of phenolic aqSOA, including $C_{16}H_{18}O_6^+$ ($m/z = 306$) for syringol dimer, $C_{14}H_{14}O_4^+$ ($m/z = 246$) for guaiacol dimer, $C_{14}H_{14}O_5^+$ ($m/z = 262$) and $C_{14}H_{14}O_6^+$ ($m/z = 278$) for hydroxylated guaiacol dimer, $C_{12}H_{10}O_2^+$ ($m/z = 186$) for phenol dimer, $C_{21}H_{20}O_6^+$ ($m/z = 368$) for guaiacol trimer, and $C_{18}H_{14}O_3^+$ ($m/z = 278$) for phenol trimer (Fig. 8). Since all these ions have odd number of electrons with relatively high m/z 's, their productions in the AMS are more directly linked to the specific parent compounds, meaning that they are less likely contributed by confounding molecules (McLafferty and Turecek, 1993). In addition, while large hydrocarbon molecules, e.g., those from vehicle emissions, may generate significant ion signals at $m/z > 200$, most of them are even-electron ions and contain no oxygen. They are therefore easily differentiated from the isobaric ions from phenolic aqSOA. Nevertheless, it is important to point out that the validity of using the signature ions identified in this study needs to be evaluated by examining ambient organic aerosol mass spectrometry data. In addition, analyzing field samples with nano-DESI may also provide important insights into the impacts of aqueous phase processing of phenolic compounds in the atmosphere.”

Reviewer #2

The authors present a detailed study of the products of aqueous-phase oxidation of phenol, guaiacol, syringol. They examine oxidation by the OH radical and by the triplet excited states of 3,4-DMB. This manuscript can be viewed as a companion paper to Smith et al., ES&T (2014). In that study the authors presented the kinetics and SOA yields of these processes, but the discussion is confined to product characterization here. The volatility and optical properties of the SOA are also examined, although these results are discussed only briefly in the manuscript.

Reviewer's comment:

1. The $^3\text{C}^*$ pathway is very interesting and potentially important. I would like to hear more from the authors regarding their choice of 3,4-DMB as a photosensitizer. Why was this model compound chosen when other aromatic carbonyl compounds exist in biomass burning aerosol which might be more environmentally relevant? Could any of the reactants (or the aromatic carbonyl products they form) also act as photosensitizers? Were any control experiments performed to investigate this?

Authors' reply #1: There are three reasons for choosing 3,4-DMB as the photosensitizer. First, 3,4-DMB has high molar absorptivities across the solar UV wavelengths and is an effective source of $^3\text{C}^*$ (Anastasio et al., 1997). Secondly, 3,4-DMB is emitted in large amounts from biomass burning (Schauer et al., 2001) and exists nearly exclusively in condensed phases in the atmosphere. Lastly, 3,4-DMB is commercially available. In response to the reviewer's comments, we added the following sentence in Sect. 2.1: "3,4-DMB was chosen as the photosensitizer in this study to represent non-phenolic aromatic carbonyls, which are emitted in large quantities from wood burning (Schauer et al., 2001), exist nearly exclusively in condensed phases in the atmosphere, and rapidly form $^3\text{C}^*$ that efficiently oxidizes phenols (Anastasio et al., 1997)."

Phenols themselves have little or no light absorption in the solar range and are not effective photosensitizers. Some of the products formed during illumination absorb light at longer wavelengths and might be photosensitizers, but we do not think that they contributed significantly to phenol loss in our experiments since the kinetics of phenol loss out to one half-life all showed good first-order decays, indicating relatively stable oxidant concentrations. For this reason, it is unlikely that intermediate species are a significant source of $^3\text{C}^*$ during the initial stage of the reaction. However, there are indications that other reactions could have become important after prolonged illumination. For example, we found that the destruction rate of guaiacol deviates from first-order decay after ~ 1.3 hours of reaction (Yu et al., in preparation). Note that the $t_{1/2}$ of guaiacol + $^3\text{C}^*$ is 35 min and all the aqSOA studied in this work were acquired at $t_{1/2}$. We will explore the influence of intermediate phenol reaction products on photosensitized chemistry in future studies. In response to the reviewer's comments, we have added relevant discussions in Sect. 2.1.

Reviewer's comment:

2. The authors propose a mechanism in Figure 7 based on their product analysis. It wasn't clear to me why the authors concluded that the $^3\text{C}^*$ exclusively oxidizes phenols directly, rather than also reacting with O_2 to producing singlet molecular oxygen (and therefore other oxidants) in the aqueous phase (e.g. Figure 4 of Smith et al. (2014))?

Authors' reply #2: The $^3\text{C}^*$ triplet can indeed react with O_2 to produce singlet oxygen (and perhaps other oxidants), which can oxidize phenols and possibly lead to the production of aqSOA. However, as we described in Smith et al. (2014), singlet molecular oxygen appears to be a negligible oxidant in our solutions because of the rapid triplet-mediated reactions. Thus we did not include this pathway in Fig. 7.

Reviewer's comment:

3. *The recent work of C. George and coworkers demonstrating SOA formation via photosensitizer chemistry (Aregahegn et al. (2013), Rossignol et al. (2014), Monge et al. (2012)) should be referenced in the introduction.*

Authors' reply #3: As suggested, we have added relevant discussions and cited these literatures in the introduction.

Reviewer's comment:

4. *Can the authors comment on the possible impacts of sample drying on the observed product distributions (e.g. oligomers and light-absorbing species)?*

Authors' reply #4: As discussed in Smith et al. (2014), there are some differences in the SOA mass yields determined gravimetrically from N₂ blowdown of solutions and those determined in real-time by HR-ToF-AMS. A possible reason is that some semi-volatile components may have reacted and formed low-volatility products during the N₂ blowdown procedure, probably because of the presence of small amount of sulfuric acid in the solution, which was added to adjust the pH of the solution (Smith et al., 2014). Despite this, according to our analysis, the ESI-MS spectra of the blown-down sample reconstituted in Milli-Q water and the flash-frozen sample for the aqSOA formed from syringol + ³C* are overall similar. For example, 65 - 70% of the molecules identified in these two sample types are common species and for both samples, oligomers and their derivatives account for ~ 50% of the total signal in the ESI spectra. In addition, the AMS spectra of the blown-down samples and those of the flash-frozen samples are overall similar. For these reasons, it appears that sample drying had relatively small influence on the observed product distribution. Nevertheless, it is important to conduct future studies to understand the reasons for these methodological differences in aqSOA yield, and evaluate the possible influence of sample drying process on aqSOA mass, composition, and light-absorbing species. In response to the reviewer's comments, we have added relevant discussions in Sect. 3.1.

References

- Anastasio, C., Faust, B. C. and Rao, C. J.: Aromatic carbonyl compounds as aqueous-phase photochemical sources of hydrogen peroxide in acidic sulfate aerosols, fogs, and clouds .1. Non-phenolic methoxybenzaldehydes and methoxyacetophenones with reductants (phenols), *Environ. Sci. Technol.*, 31, 218-232, doi:10.1021/es960359g, 1997.
- Anastasio, C. and McGregor, K. G.: Chemistry of fog waters in California's Central Valley: 1. In situ photoformation of hydroxyl radical and singlet molecular oxygen, *Atmos. Environ.*, 35, 1079-1089, doi:10.1016/s1352-2310(00)00281-8, 2001.
- Arakaki, T., Anastasio, C., Kuroki, Y., Nakajima, H., Okada, K., Kotani, Y., Handa, D., Azechi, S., Kimura, T., Tshako, A. and Miyagi, Y.: A General Scavenging Rate Constant for Reaction of Hydroxyl Radical with Organic Carbon in Atmospheric Waters, *Environ. Sci. Technol.*, 47, 8196-8203, doi:10.1021/es401927b, 2013.
- Dzepina, K., Arey, J., Marr, L. C., Worsnop, D. R., Salcedo, D., Zhang, Q., Onasch, T. B., Molina, L. T., Molina, M. J. and Jimenez, J. L.: Detection of particle-phase polycyclic aromatic hydrocarbons in Mexico City using an aerosol mass spectrometer, *Int. J. Mass Spectrom.*, 263, 152-170, doi:10.1016/j.ijms.2007.01.010, 2007.
- Farmer, D. K., Matsunaga, A., Docherty, K. S., Surratt, J. D., Seinfeld, J. H., Ziemann, P. J. and Jimenez, J. L.: Response of an aerosol mass spectrometer to organonitrates and organosulfates and

- implications for atmospheric chemistry, *Proc. Natl. Acad. Sci.*, 107, 6670-6675, doi:10.1073/pnas.0912340107, 2010.
- Ge, X., Setyan, A., Sun, Y. and Zhang, Q.: Primary and secondary organic aerosols in Fresno, California during wintertime: Results from high resolution aerosol mass spectrometry, *J. Geophys. Res.*, 117, D19301, doi:10.1029/2012JD018026, 2012.
- Ge, X., Shaw, S. L. and Zhang, Q.: Toward understanding amines and their degradation products from postcombustion CO₂ capture processes with aerosol mass spectrometry, *Environ. Sci. Technol.*, 48, 5066-5075, doi:10.1021/es4056966, 2014.
- McLafferty, F. W. and Turecek, F.: *Interpretation of Mass Spectra*, University Science Books, Mill Valley, California, 1993.
- Nguyen, T. B., Nizkorodov, S. A., Laskin, A. and Laskin, J.: An approach toward quantification of organic compounds in complex environmental samples using high-resolution electrospray ionization mass spectrometry, *Anal. Methods*, 5, 72-80, doi:10.1039/c2ay25682g, 2013.
- Schauer, J. J., Kleeman, M. J., Cass, G. R. and Simoneit, B. R. T.: Measurement of emissions from air pollution sources. 3. C-1-C-29 organic compounds from fireplace combustion of wood, *Environ. Sci. Technol.*, 35, 1716-1728, doi:10.1021/es001331e, 2001.
- Smith, J. D., Sio, V., Yu, L., Zhang, Q. and Anastasio, C.: Secondary organic aerosol production from aqueous reactions of atmospheric phenols with an organic triplet excited state, *Environ. Sci. Technol.*, 48, 1049-1057, doi:10.1021/es4045715, 2014.
- Ulbrich, I. M., Canagaratna, M. R., Zhang, Q., Worsnop, D. R. and Jimenez, J. L.: Interpretation of organic components from Positive Matrix Factorization of aerosol mass spectrometric data, *Atmos. Chem. Phys.*, 9, 2891-2918, doi:10.5194/acp-9-2891-2009, 2009.
- Zhang, Q., Alfarra, M. R., Worsnop, D. R., Allan, J. D., Coe, H., Canagaratna, M. R. and Jimenez, J. L.: Deconvolution and quantification of hydrocarbon-like and oxygenated organic aerosols based on aerosol mass spectrometry, *Environ. Sci. Technol.*, 39, 4938-4952, doi:10.1021/es0485681, 2005.
- Zhang, Q., Jimenez, J., Canagaratna, M., Ulbrich, I., Ng, N., Worsnop, D. and Sun, Y.: Understanding atmospheric organic aerosols via factor analysis of aerosol mass spectrometry: a review, *Anal. Bioanal. Chem.*, 401, 3045-3067, doi:10.1007/s00216-011-5355-y, 2011.

1 **Chemical characterization of SOA formed from aqueous-phase reactions of phenols with**
2 **the triplet excited state of carbonyl and hydroxyl radical**

3
4 Lu Yu¹, Jeremy Smith², Alexander Laskin³, Cort Anastasio², Julia Laskin⁴, Qi Zhang^{1*}

5 ¹Department of Environmental Toxicology, University of California, 1 Shields Ave., Davis, CA
6 95616, USA

7 ²Department of Land, Air and Water Resources, University of California, 1 Shields Ave., Davis,
8 CA 95616, USA

9 ³Environmental Molecular Sciences Laboratory, Pacific Northwest National Laboratory,
10 Richland, WA 99352, USA

11 ⁴Physical Sciences Division, Pacific Northwest National Laboratory, Richland, WA 99352, USA

12
13 *Corresponding Author: Qi Zhang, Department of Environmental Toxicology, University of
14 California, 1 Shields Ave., Davis, CA 95616, USA. Tel.: 530-752-5779; fax: 530-752-3394; e-
15 mail: dkwzhang@ucdavis.edu

18 **Abstract**

19 Phenolic compounds, which are emitted in significant amounts from biomass burning,
20 can undergo fast reactions in atmospheric aqueous phases to form secondary organic aerosol
21 (aqSOA). In this study, we investigate the reactions of phenol and two methoxy-phenols
22 (syringol and guaiacol) with two major aqueous phase oxidants – the triplet excited states of an
23 aromatic carbonyl ($^3C^*$) and hydroxyl radical ($\bullet OH$). We thoroughly characterize the low-
24 volatility species produced from these reactions and interpret their formation mechanisms using
25 aerosol mass spectrometry (AMS), nanospray desorption electrospray ionization mass
26 spectrometry (nano-DESI MS), and ion chromatography (IC). A large number of oxygenated
27 molecules are identified, including oligomers containing up to six monomer units, functionalized
28 monomer and oligomers with carbonyl, carboxyl, and hydroxyl groups, and small organic acid
29 anions (e.g., formate, acetate, oxalate, and malate). The average atomic oxygen-to-carbon (O/C)
30 ratios of phenolic aqSOA are in the range of 0.85-1.23, similar to those of low-volatility
31 oxygenated organic aerosol (LV-OOA) observed in ambient air. The aqSOA compositions are
32 overall similar for the same precursor, but the reactions mediated by $^3C^*$ are faster than $\bullet OH$ -
33 mediated reactions and produce more oligomers and hydroxylated species at the point when 50%
34 of the phenol had reacted. Profiles determined using a thermodenuder indicate that the volatility
35 of phenolic aqSOA is influenced by both oligomer content and O/C ratio. In addition, the aqSOA
36 shows enhanced light absorption in the UV-vis region, suggesting that aqueous-phase reactions
37 of phenols ~~are likely an important source of~~ may contribute to formation of secondary brown
38 carbon in the atmosphere, especially in regions influenced by biomass burning.

39 Keywords: phenol, guaiacol, syringol, particulate matter, hydroxyl radical, $^3C^*$, SOA
40 formation mechanisms, aqSOA

41 1. Introduction

42 Secondary organic aerosol (SOA) is ubiquitous in the atmosphere (Murphy et al., 2006;
43 Zhang et al., 2007; Jimenez et al., 2009) and plays an important role in climate, human health,
44 and air quality. Thus, understanding the impacts of SOA requires a thorough knowledge of the
45 formation, evolution, and composition of SOA. This knowledge, however, is still limited because
46 atmospheric organic chemistry is extremely complex. Numerous sources emit organic
47 compounds and organic aerosol is formed and transformed via complicated chemical and
48 physical processes in the atmosphere (Kanakidou et al., 2005).

49 SOA formation can take place in both gas and condensed phases. Much of the previous
50 research on SOA has mainly focused on gas-phase reactions of volatile organic compounds
51 (Hallquist et al., 2009). Recent work, however, has shown that SOA can also be produced
52 efficiently in cloud and fog drops and water-containing aerosol (Blando and Turpin, 2000; Lim
53 et al., 2005; Altieri et al., 2006; Ervens et al., 2011). Understanding the characteristics of SOA
54 formed from aqueous-phase reactions (aqSOA) is important for properly representing its
55 formation pathways in models and for elucidating its climatic and health effects.

56 Phenols are important precursors of aqSOA because 1) they are emitted in large
57 quantities from biomass burning (Hawthorne et al., 1989; Schauer et al., 2001); 2) they have high
58 Henry's Law constants and can partition significantly into atmospheric aqueous phases (Sagebiel
59 and Seiber, 1993; Sander, 1999); and 3) they can undergo fast reactions with hydroxyl radical
60 ($\bullet\text{OH}$) and triplet excited states of organic compounds ($^3\text{C}^*$) formed via light absorption by
61 dissolved chromophores (Anastasio et al., 1997; Canonica et al., 2000; Smith et al., 2014). In the
62 aqueous phase, $\bullet\text{OH}$ is typically considered a dominant oxidant for organics. However, a recent
63 study by Smith et al. (2014) showed that the destruction rates of phenols by $^3\text{C}^*$ are comparable

64 to or faster than those by •OH under typical ambient conditions in areas influenced by biomass
65 burning. An important source of $^3\text{C}^*$ in the atmosphere is non-phenolic aromatic carbonyls – a
66 group of compounds that are emitted from wood combustion in significant amounts (Hawthorne
67 et al., 1992; Simoneit et al., 1999) and have been detected in fog and cloud droplets
68 (Leuenberger et al., 1985; Sagebiel and Seiber, 1993). These compounds, once dissolved in
69 water, can absorb light to form $^3\text{C}^*$ and catalyze the photooxidationoxidation of phenols~~and~~
70 generate aqSOA with little or no loss of the aromatic carbonyl (Anastasio et al., 1997; Smith et
71 al., 2014). This is an indication that non-phenolic aromatic carbonyls, along with a number of
72 other organic compounds recently reported (Monge et al., 2012; Aregahegn et al., 2013;
73 Rossignol et al., 2014), can act as photosensitizer to promote SOA formation in atmospheric
74 condensed phases.

75 RecentAccording to recent studies ~~have shown that~~, phenols react with •OH and $^3\text{C}^*$ to
76 form aqSOA with mass yields close to 100% (Smith et al., 2014)~~and that the, making~~ reaction
77 products that include small organic acids, hydroxylated phenols, and oligomers (Sun et al., 2010).
78 However, since Sun et al. (2010) mainly used an Aerodyne high-resolution time-of-flight aerosol
79 mass spectrometer with an electron impact (EI) ionization source, in which analyte molecules are
80 generally extensively fragmented (Canagaratna et al., 2007), the molecular composition of the
81 phenolic aqSOA was not sufficiently characterized. ~~In addition~~In addition, since Sun et al. (2010)
82 examined phenol reactions only with •OH, almost nothing is known about the chemistry of
83 aqSOA formed from $^3\text{C}^*$ reactions.

84 In this study, we thoroughly characterize the aqueous reaction products of phenols with
85 $^3\text{C}^*$ produced from a non-phenolic aromatic carbonyl and •OH from hydrogen peroxide (HOOH)
86 under simulated sunlight illumination. We studied three basic structures of biomass-burning

87 phenols – phenol (C₆H₆O), guaiacol (C₇H₈O₂; 2-methoxyphenol), and syringol (C₈H₁₀O₃; 2,6-
88 dimethoxyphenol). We examine the molecular and bulk compositions of low-volatility species
89 produced from these reactions and use this information to interpret the formation pathways of
90 phenolic aqSOA.

91 **2. Experimental Methods**

92 *2.1 Phenolic aqSOA samples*

93 The aqSOA samples of phenol, guaiacol, and syringol were prepared during simulated
94 sunlight illumination under two oxidant conditions: (1) via reaction with ³C* formed from 5 ~~μM~~
95 ~~3,4-dimethoxybenzaldehyde (3,4-DMB) and (2) via reaction with •OH generated from 100 μM~~
96 ~~hydrogen peroxide (HOOH; Table 1). Details of the experiments are given in Smith et al.~~
97 ~~(2014)~~ μmol L⁻¹ 3,4-dimethoxybenzaldehyde (3,4-DMB) and (2) via reaction with •OH generated
98 from 100 μmol L⁻¹ hydrogen peroxide (HOOH; Table 1). 3,4-DMB was chosen as the
99 photosensitizer in this study to represent non-phenolic aromatic carbonyls, which are emitted in
100 large quantities from wood burning (Schauer et al., 2001), exist nearly exclusively in condensed
101 phases in the atmosphere, and rapidly form ³C* that efficiently oxidizes phenols (Anastasio et al.,
102 1997). Details of the experiments are reported in Smith et al. (2014) and a brief summary is
103 given here. Initial solutions were composed of air-saturated Milli-Q water (resistance > 18 MΩ-
104 cm; Millipore) containing 100 μmol L⁻¹ of a single phenol and adjusted to pH = 5 using
105 sulfuric acid. Each solution was illuminated in an RPR-200 Photoreactor System (George et al.,
106 2014) until approximately half of the initial phenol was degraded (as monitored by a high
107 performance liquid chromatograph (HPLC) with a UV-vis detector). At that point, 12.0 mL of
108 the illuminated solution was placed in an aluminum cup and blown gently to dryness with pure
109 N₂ at room temperature. Another aliquot of the illuminated solution was flash frozen with liquid

110 | nitrogen and stored at - 20 °C in the dark until analysis. Note that the flash-frozen samples
111 | contain dissolved volatile species, low-volatility species and unreacted precursors, while the
112 | blown-down samples are composed of only low-volatility species. Indeed, HPLC analysis of the
113 | blown-down samples detected negligible amounts of the initial phenols, indicating that they were
114 | completely removed. In addition, all phenolic precursors show first-order decay during
115 | photoreactions to a time of one half-life (Smith et al., 2014), indicating that the reaction
116 | intermediates or products are not acting as significant photosensitizers. The phenol precursors
117 | themselves are not effective photosensitizers since they have little or no light absorption in the
118 | solar range (Smith et al., 2014). Dark control experiments, carried out under the same condition
119 | except in the dark, showed negligible loss of phenol and no formation of aqSOA. In addition, no
120 | formation of aqSOA was observed in control experiments in which 3,4-DMB was illuminated
121 | alone under the same condition and the resulting solution evaporated in the same way.

122 | ***2.2 Analytical methods***

123 | *2.2.1 Aerosol Mass Spectrometry (AMS) measurement and data analysis*

124 | In this study, a High Resolution Time-of-Flight Aerosol Mass Spectrometer (Aerodyne
125 | Res. Inc., Billerica, MA; thereafter referred to as AMS) was used to characterize the bulk
126 | chemical composition and elemental ratios of the low-volatility substances in both blown-down
127 | and flash-frozen samples. The working principles of the AMS have been discussed previously
128 | (DeCarlo et al., 2006; Canagaratna et al., 2007). Briefly, the AMS analyzes nonrefractory
129 | aerosols that ~~can be evaporated~~evaporate at ~ 600 °C under high vacuum via 70 eV EI mass
130 | spectrometry. In this study, the AMS was operated alternatively between “V” and “W” ion
131 | optical modes (mass resolutions of ~ 3000 and ~ 5000, respectively) to acquire mass spectra up
132 | to m/z 500 and m/z 300, respectively. Prior to AMS analysis, each blown-down sample was

133 dissolved in 6.0 mL Milli-Q water and the flash-frozen samples were thawed overnight inside a
134 refrigerator (~ 4 °C). The liquid samples were atomized in argon (Industrial Grade, 99.997%)
135 using a constant output atomizer coupled with a diffusion dryer and the resulting particles were
136 analyzed by the AMS downstream of a digitally controlled thermodenuder (TD) (Fierz et al.,
137 2007). The TD consists of a bypass line and a heated line terminating in a section with activated
138 carbon cloth. The temperature inside the heated line was programmed to cycle through 7
139 different temperatures (25, 40, 65, 85, 100, 150, and 200 °C) every hour. An automated 3-way
140 valve switched the sample flow between bypass and TD modes every 5 min. By comparing the
141 measurements between these two modes, we can determine the volatility profiles of the aqSOA.
142 Between every two sample runs, Milli-Q water was atomized and analyzed as an analytical blank.

143 The AMS data were analyzed using the AMS data analysis software (SQUIRREL v1.12
144 and PIKA v1.53 downloaded from [http://cires.colorado.edu/jimenez-](http://cires.colorado.edu/jimenez-group/ToFAMSResources/ToFSoftware/)
145 [group/ToFAMSResources/ToFSoftware/](http://cires.colorado.edu/jimenez-group/ToFAMSResources/ToFSoftware/)). The W-mode data was analyzed to determine the
146 atomic ratios of oxygen-to-carbon (O/C) and hydrogen-to-carbon (H/C) and the organic mass-to-
147 carbon ratio (OM/OC) of phenolic aqSOA (Aiken et al., 2008). V-mode data were analyzed for
148 information of higher molecular weight ions with $m/z > 300$, such as syringol dimer $C_{16}H_{18}O_6^+$
149 (m/z 306) and guaiacol trimer $C_{21}H_{20}O_6^+$ (m/z 368). Note that accurately quantifying the organic
150 contributions to the H_2O^+ , CO^+ , and CO_2^+ signals in an ensemble mass spectrum is critical to the
151 determination of the O/C and H/C ratios of an organic aerosol (Aiken et al., 2008; Sun et al.,
152 2009; Collier and Zhang, 2013). Since Ar was used as the carrier gas for atomization, N_2 and
153 CO_2 did not interfere with the quantification of the organic CO^+ and CO_2^+ signals. In terms of the
154 H_2O^+ signal, contribution from gaseous water molecules was negligible because the relative
155 humidity measured at the AMS inlet was very low ($< 2\%$). In addition, since heating the aerosol

156 to 40 °C prior to AMS sampling led to almost no change in the relative intensities of the H₂O⁺
157 signal in the mass spectra of aqSOA (Fig. S1 in the supplementary information), particles
158 appeared to be completely dry. The organic portion of the H₂O⁺ signal was thus determined as
159 the difference between the measured H₂O⁺ signal and the sulfate-associated H₂O⁺ signal
160 estimated according to the known fragmentation pattern of sulfates (Allan et al., 2004).

161 *2.2.2 Nanospray Desorption Electrospray Ionization Mass Spectrometry (nano-DESI MS)* 162 *measurement and data analysis*

163 Prior to nano-DESI MS analysis, the blown-down samples of phenolic aqSOA were
164 dissolved in Milli-Q water, atomized, and collected on Teflon membrane filters. The analyses
165 were performed using a high-resolution LTQ-Orbitrap mass spectrometer (Thermo Electron,
166 Bremen, Germany) with a resolving power ($m/\Delta m$) of 100,000 at $m/z = 400$. The instrument is
167 equipped with a nano-DESI source assembled from two fused-silica capillaries (150 μm o.d./50
168 μm i.d.) (Roach et al., 2010b). Analyte molecules extracted into the liquid bridge formed
169 between the two capillaries are transferred to a mass spectrometer inlet and ionized by
170 nanoelectrospray. The analysis was performed under the following conditions: spray voltage of
171 3-5 kV, 0.5-1 mm distance from the tip of the nanospray capillary to the 300 °C heated inlet of
172 the LTQ-Orbitrap, and 0.3-0.9 $\mu\text{L}/\text{min}$ flow rate of acetonitrile : water (1:1 volume) solvent. The
173 instrument was calibrated using a standard mixture of caffeine, MRFA (met-arg-phe-ala) peptide,
174 and Ultramark 1621 (Thermo Scientific, Inc.) for the positive ion mode and a standard mixture
175 containing sodium dodecyl sulfate, sodium taurocholate, and Ultramark 1621 (Thermo Scientific,
176 Inc.) for the negative ion mode. Both positive and negative mode mass spectra were acquired
177 using the Xcalibur software (Thermo Electron, Inc.). To analyze a sample, the nano-DESI probe

178 was first placed on a clean area of the filter to record the background signal for ~ 3min and then
179 positioned on the sample region to acquire data for an additional 4-5min (Roach et al., 2010a).

180 Peaks with S/N > 10 were selected using the Decon2LS software developed at the Pacific
181 Northwest National Laboratory (PNNL) (Jaitly et al., 2009). Further data processing was
182 performed with Microsoft Excel using a set of built-in macros developed by Roach et al. (2011).
183 The background and sample peaks were aligned, and the peaks corresponding to ¹³C isotopes
184 were removed. Only peaks in the sample spectra that are at least 10 times bigger than the
185 corresponding peaks in the background spectra were retained for further analysis. Peaks were
186 segregated into different groups using the higher-order mass defect transformation developed by
187 Roach et al. (2011). Specifically, the peaks were first grouped using a CH₂-based transformation
188 and then an H₂-based second-order transformation. Formula Calculator v. 1.1
189 (http://www.magnet.fsu.edu/usershub/scientificdivisions/icr/icr_software.html) was then used to
190 assign the molecular formula to each group using the following constraints: C ≥ 0, H ≥ 0, O ≥ 0
191 for the negative ion mode data and C ≥ 0, H ≥ 0, O ≥ 0, Na ≤ 1 for the positive ion mode data.
192 Approximately 70% of the peaks were assigned with molecular formula within these constraints.
193 The formulas of neutral species were subsequently determined by removing the adduct ion (e.g.,
194 a proton or a sodium ion) from the positive ions or by adding a proton to the negative ions.

195 Kendrick representation of high resolution mass spectral data can be used to search for
196 potential oligomeric units (Hughey et al., 2001). In this study, O-based Kendrick diagram was
197 used to investigate the degree of hydroxylation. The Kendrick mass (KM) and Kendrick mass
198 defect (KMD) are calculated using the following two equations:

$$199 \quad \text{KM} = \text{observed mass} \times 16 / 15.9949 \quad (1)$$

$$200 \quad \text{KMD} = \text{NM} - \text{KM} \quad (2)$$

201 Where, 16 is the nominal mass of O, 15.9949 is the exact mass of the O, and NM is the KM
202 rounded to the nearest integer. Plotting KMD versus KM reveals homologous series of
203 compounds differing only by the number of base units which fall on horizontal lines.

204 Double bond equivalent (DBE) indicates the number of double bonds and rings in a
205 closed-shell organic molecule (Pellegrin, 1983). For a molecule with a nominal formula of
206 $C_xH_yO_z$ (where x , y , z denote the number of C, H, and O atoms, respectively, in the molecule),
207 $DBE = 1 - y/2 + x$.

208 *2.2.3 Ion Chromatography (IC) and Total Organic Carbon (TOC) analysis*

209 Concentrations of inorganic/organic anions were measured using an ion chromatograph
210 (Metrohm 881 Compact IC Pro, Switzerland) equipped with an autosampler, a Metrosep RP2
211 guard/3.6 column and a Metrosep A Supp15 250/4.0 column, and a conductivity detector. Details
212 on the IC method are given in Ge et al. (2014). Briefly, anions were eluted at 0.8 ml/min using
213 an eluent of 5 ~~mM~~mmol L⁻¹ Na₂CO₃ and 0.3 ~~mM~~mmol L⁻¹ NaOH in water. This method can
214 separate and quantify 9 organic anions (glycolate, formate, acetate, pyruvate, oxalate, malate,
215 malonate, maleate, and fumarate) and 7 inorganic anions (F⁻, Cl⁻, NO₂⁻, Br⁻, NO₃⁻, SO₄²⁻ and
216 PO₄³⁻). The IC results were evaluated in terms of reproducibilities of retention times and peak
217 heights and linearity of the calibration curves. Analysis of external check standards, including a
218 7-anion standard mixture (Dionex) and 4 individual standards (Metrohm), always produced
219 results that were within 10% of certified values. Relative differences for replicate analyses were
220 within 3%.

221 A Shimadzu TOC-VCPH analyzer was applied to measure TOC in the aqSOA samples.
222 The instrument uses a combustion tube filled with oxidation catalyst to convert all carbon atoms
223 into CO₂ at 720 °C under ultrapure air and quantifies the resulting CO₂ using a non-dispersive

224 infrared (NDIR) analyzer. Prior to combustion, inorganic carbon species
225 (carbonates/bicarbonates and dissolved CO₂) is transformed into CO₂ by 25% H₃PO₄, bubbled
226 out, and determined by NDIR. TOC is determined as the difference. The TOC analyzer was
227 calibrated using the standard solutions of NaHCO₃, Na₂CO₃, and potassium hydrogen phthalate
228 (Sigma-Aldrich or Wako-Japan, ≥ 99.0%). Results from external TOC check standards (Aqua
229 Solutions) were always within 10% of certified values.

230 3. Results and discussion

231 3.1 Overview of the chemical characteristics of phenolic aqSOA

232 The lifetime of phenols with respect to ³C* and •OH reactions in atmospheric fog and
233 cloud water is on the order of minutes to hours during daytime (Smith et al., 2014). Compared to
234 •OH, ~~the reaction rates of~~ ³C* ~~reacts more quickly~~ with phenols ~~are faster~~, but the mass yields of
235 aqSOA from both reactions are near 100% for phenol, guaiacol, and syringol (Smith et al.,
236 2014). ~~The reaction rate comparisons in this manuscript are based on the experimentally~~
237 ~~measured pseudo first-order rate constants for phenol loss (k'_{ArOH}), which are equal to the~~
238 ~~product of the bimolecular rate constant and steady state concentration of oxidant: $k'_{ArOH} =$~~
239 ~~$k_{ArOH+Oxidant}[Oxidant]$ (Smith et al., 2014). Based on bimolecular rate constants determined by~~
240 ~~Smith et al. (in preparation), the steady-state concentrations of •OH and ³C* during this study are~~
241 ~~estimated at $10^{-16} \sim 10^{-15}$ mol L⁻¹ and $\sim 10^{-14}$ mol L⁻¹, respectively, which are similar to the typical~~
242 ~~aqueous •OH concentration in fog and cloud waters (Anastasio and McGregor, 2001; Arakaki et~~
243 ~~al., 2013) and the ³C* concentration measured in Davis fog waters (R. Kaur, unpublished results).~~

244 As shown in Fig. 1 and summarized in Table 1, the aqSOA formed from all three phenols
245 with both oxidants are highly oxygenated ~~with average O/C ratios in the range of 0.85-1.23,~~
246 ~~with average O/C ratios in the range of 0.85-1.23 and average organic mass to carbon ratios~~

247 [\(OM/OC\) in the range of 2.27-2.79. Based on a comparison to the OM/OC of the precursors, the](#)
248 [mass yields of the aqSOA should be 142 - 214%, assuming all reacted phenols were converted](#)
249 [into low volatility species. However, the measured values are 16-38% lower, indicating that](#)
250 [approximately 16-38% of the reacted phenols were converted into volatile and semi-volatile](#)
251 [species that evaporated during illumination and/or drying.](#) These results are consistent with a
252 previous study by Sun et al. (2010), where O/C ratios of phenolic aqSOA formed from direct
253 photodegradation and •OH oxidation were in the range of 0.80-1.06. The O/C of phenolic SOA
254 from gas-phase •OH oxidation are also near unity (Chhabra et al., 2011; Yee et al., 2013). Due to
255 high oxygen contents, the organic mass-to-carbon (OM/OC) ratios of the aqSOA are high
256 (average = 2.27-2.79; Table 1). Note that the OM/OC ratios determined by AMS agree well with
257 those determined based on aqSOA mass measured gravimetrically and organic carbon mass
258 measured by a TOC analyzer (Fig. S2). For the same oxidant, the O/C ratio of the aqSOA formed
259 at $t_{1/2}$ follows the order: phenol > guaiacol > syringol (Table 1). This trend is likely driven by
260 precursor reactivity, which determines how long the solution needed to be illuminated to reach
261 one half-life, and has the order: syringol > guaiacol > phenol. [The reactivity differences among](#)
262 [the three precursors are likely due to the electron-donating effect of the o-methoxy substituents,](#)
263 [which may increase the rate of electrophilic reactions on the benzene ring.](#) Longer illumination
264 time increases the formation of highly oxygenated species and ~~smaller~~-ring-opening species- ([nC](#)
265 [≤ 6](#)). For the same reason, •OH oxidation, which is slower than $^3\text{C}^*$ reaction for the same phenol
266 precursor, generally produces more oxidized aqSOA at $t_{1/2}$.

267 Figures S3 and S4 show the nano-DESI MS spectra of the aqSOA of syringol, guaiacol,
268 and phenol formed from $^3\text{C}^*$ and •OH reactions, respectively. Hundreds of species were
269 identified, all of which are oxygenated with the median O/C ratios of the molecules varying from

270 0.33-0.55 in different aqSOA samples (Fig. 1). The signal-weighted average O/C ratios
271 (Bateman et al., 2012) of phenolic aqSOA are in the range of 0.31-0.65 according to the negative
272 ion mode nano-DESI results, which are ~~significantly lower than the average O/C of bulk aqSOA~~
273 ~~measured by the AMS (Fig. 1). This discrepancy may be attributed to lower electrospray~~
274 ~~ionization efficiencies of some highly oxidized species or the dissociation of quasi-molecular~~
275 ~~ions which leads to the loss of highly oxygenated moieties (e.g., loss of CO₂ for aromatic~~
276 ~~carboxylic acids) in nano-DESI analysis (Levsen et al., 2007). In addition, in order to provide~~
277 ~~better coverage of high-mass ions, nano-DESI mass spectra were analyzed only for ions with~~
278 ~~$m/z > 100$. Therefore, high O/C species with molecular weight lower than 100 dalton (Da), such~~
279 ~~as oxalate (O/C = 2), formate (O/C = 1), and pyruvate (O/C = 1), were not observed in our nano-~~
280 ~~DESI experiments. According to IC analysis, these small organic anions together represent 0.8-~~
281 ~~3.8% of the TOC of aqSOA (Table 1).~~ systematically lower than the average O/C of bulk aqSOA
282 measured by the AMS (Fig. 1). However, due to large differences between the AMS and the
283 nano-DESI methodology, in terms of sample analysis, data processing, and assumptions used for
284 average O/C calculations, a direct comparison between these two sets of O/C data should be
285 cautioned.

286 Figure 2 shows the AMS spectra of different aqSOA acquired after 50% of the initial
287 phenols had reacted (i.e., at $t_{1/2}$). A prominent feature of these spectra is that CO₂⁺ ($m/z = 44$),
288 H₂O⁺ ($m/z = 18$), and CO⁺ ($m/z = 28$) are the largest peaks, similar to the spectral pattern of fulvic
289 acid – a model compound representative of highly processed and oxidized organic particulate
290 matter and humic-like substances (HULIS) (Zhang et al., 2005; Ofner et al., 2011). The AMS
291 spectra of syringol aqSOA formed from different oxidants are almost identical (Fig. 2),
292 indicating similar chemical compositions. Similarly, nano-DESI analysis shows the formation of

293 a large number of common species, i.e., 883 species with common elemental composition (Table
294 1), through the reactions of syringol with $^3\text{C}^*$ and $\bullet\text{OH}$, which account for 76% and 88%,
295 respectively, of the total number of molecules identified in the corresponding aqSOA. A similar
296 overlap of common species was observed for guaiacol aqSOA. But the molecular compositions
297 of phenol aqSOA are more different between the two oxidants (Table 1), which is consistent with
298 the fact that the AMS spectra of the two phenol aqSOA are largely different at $m/z \geq 80$ (Fig. 2I).
299 The more distinct compositional differences of phenol aqSOA between the $\bullet\text{OH}$ and $^3\text{C}^*$
300 reactions is probably due to the larger difference in reaction times (i.e., $t_{1/2} = 672$ min vs. 480
301 min; Table 1). Detailed discussions on the comparisons of aqSOA produced from the same
302 precursor but different oxidants are given in Sect. 3.3.

303 A total number of 149 common molecules were identified in all samples (Table 1).
304 Figure 3 shows the Van Krevelen diagram of these common molecules. A majority of these
305 molecules have molecular weight lower than 400 Da and DBE < 12 (Fig. 3), indicating that they
306 contain two or less aromatic rings and that they were likely produced from ring-opening
307 reactions. In addition, small carboxylate anions were observed in all aqSOA samples, although
308 they represent only a small fraction of the TOC (Table 1). It is interesting to point out that the
309 number of molecules observed by nano-DESI decreases with increasing illumination time across
310 all 3 phenols, suggesting that increased aging simplifies the products to a smaller set (Table 1).
311 However, this trend could also be related to ionization efficiency of different types of phenolic
312 aqSOA. For example, syringol aqSOA has more methoxy groups, thus is easier to get ionized by
313 nano-DESI, compared to phenol aqSOA.

314 Both flash-frozen (FF) and blown-down (BD) samples were chemically characterized and
315 | show almost identical AMS spectra (Fig. S5). [This is a confirmation](#) [We also found that the ESI-](#)

316 [MS spectra of the aqueous solution of the blown-down sample and the flash-frozen sample for](#)
317 [the aqSOA formed from syringol + \$^{13}\text{C}^*\$ are also overall similar. These observations confirm](#) that
318 the non-volatile components of these two sample types are chemically very similar, [and the](#)
319 [blown-down procedure had relatively small influence on the observed product distribution.](#) Since
320 FF samples contain dissolved volatile species which should have evaporated during nebulization
321 and drying, we estimated the amount of these species by examining the differences in the TOC
322 concentrations between FF and BD samples after correction for the mass of unreacted precursors.
323 Figure 4 shows the contributions of reactants (phenolic precursor and DMB) and products
324 (dissolved volatile species and aqSOA) to the solution TOC after illumination to $t_{1/2}$. Dissolved
325 volatile species formed during photolysis represent a small fraction (2.7 - 6.6%; Table 1) of the
326 total carbon originally present in the reactants, consistent with the high mass yields of phenolic
327 aqSOA reported by Smith et al. (2014).

328 ***3.2 Insights into aqSOA formation mechanisms***

329 In this section we synthesize the molecular composition and bulk chemistry results and
330 interpret the formation mechanisms of phenolic aqSOA. A notable result is the large number of
331 dimer and higher oligomers (up to hexamer) found in the aqSOA. As shown in Figures S3 and
332 S4, the nano-DESI MS spectra of phenolic aqSOA contain clearly distinguished regions
333 corresponding to monomers, dimers, trimers, tetramers, pentamers, and hexamers and their
334 oxidation products. We therefore determine the distributions of phenolic aqSOA species based
335 on the degree of oligomerization by summing signals in each region (Fig. 5). Oligomers and
336 related derivative species clearly account for a significant fraction (24.2% - 92.6%) of the total
337 signals in the nano-DESI spectra of all phenolic aqSOA. Substituted monomers and ~~smaller~~ ring-

338 | opening species ($n_C < 6$) are also present in all aqSOA and they are particularly abundant in that
339 | of phenol + $\bullet\text{OH}$.

340 | Table 2 lists the 10 most abundant compounds identified in the aqSOA of syringol
341 | formed through reaction with $\bullet\text{OH}$ or $^3\text{C}^*$. Among them 7 are common species, including
342 | syringol dimer ($\text{C}_{16}\text{H}_{18}\text{O}_6$), hydroxylated syringol ($\text{C}_8\text{H}_{10}\text{O}_5$), three dimer derivatives ($\text{C}_{15}\text{H}_{14}\text{O}_6$,
343 | $\text{C}_{15}\text{H}_{16}\text{O}_6$ and $\text{C}_{15}\text{H}_{16}\text{O}_9$), and two monomer derivatives ($\text{C}_{15}\text{H}_{18}\text{O}_7$ and $\text{C}_{12}\text{H}_{12}\text{O}_7$). Guaiacol
344 | aqSOA is also dominated by the dimer and related species whereas substituted monomers are
345 | more abundant in phenol aqSOA (Fig. 5). The presence of dimers and substituted monomers is
346 | also evident in the AMS spectra. As an example, Figure 6 shows the AMS spectra of phenol
347 | aqSOA along with the NIST mass spectra of possible products. The spectra of guaiacol and
348 | syringol aqSOA are shown in Figures S6 and S7. Note that the AMS spectrum of biphenyl-4,4'-
349 | diol – a substituted phenolic compound – is very similar to the NIST mass spectrum (Fig. S8),
350 | indicating the validity of interpreting the AMS spectra of the phenolic aqSOA based on the NIST
351 | spectra of possible products. The AMS spectra of phenol aqSOA show a prominent peak at $m/z =$
352 | 186 ($\text{C}_{12}\text{H}_{10}\text{O}_2^+$), which is the molecular ion (M^+) of phenol dimer (Fig. 6). Similarly, the
353 | molecular ion of guaiacol dimer ($\text{C}_{14}\text{H}_{14}\text{O}_4^+$; $m/z = 246$; Fig. S6) is also noticeable in the AMS
354 | spectra. These results indicate that oligomerization is an important aqueous-phase reaction
355 | pathway that leads to the formation of aqSOA from phenols.

356 | Hydroxylation is another important reaction pathway that forms and transforms phenolic
357 | aqSOA. As shown in Figure S9, the O-based Kendrick diagram of syringol aqSOA clearly
358 | indicates the presence of a large number of species with different degrees of hydroxylation.
359 | Similarly, AMS analysis reveals the ubiquitous formation of hydroxylated products as well. For
360 | example, the AMS spectra of phenol aqSOA show prominent peaks at $m/z = 110$ ($\text{C}_6\text{H}_6\text{O}_2^+$) and

361 $m/z = 202$ ($C_{12}H_{10}O_3^+$), suggesting the presence of hydroxylated phenol and hydroxylated phenol
362 dimer, respectively (Fig. 6). In addition, signature ions representing 2-methoxyhydroquinone are
363 detected in guaiacol aqSOA (Fig. S6) and 3,4,5-trihydroxy benzoic acid is likely a product of
364 syringol oxidation (Fig. S7)

365 Both nano-DESI and AMS results further reveal the broad formation of aldehydes, esters,
366 and carboxylated products. As shown in Table 2, $C_9H_{10}O_4$ (MW = 182; DBE = 5), which was
367 found to present at high abundance in the aqSOA of syringol + $^3C^*$, is likely a syringol aldehyde.
368 In addition, the pronounced $C_7H_5O_2^+$ ($m/z = 121$) peak in the AMS spectra of phenol aqSOA (Fig.
369 6a) indicates the formation of phenol esters such as methylparaben and ethylparaben (Fig. 6d)
370 and the prominent $C_8H_7O_3^+$ ($m/z = 151$) signal in the guaiacol aqSOA spectra (Fig. S6a) suggests
371 the formation of a guaiacol ester – methyl vanillate (Fig. S6c).

372 Small organic acid anions (i.e., formate, acetate, oxalate, malate, malonate, etc.) are
373 observed in all samples and these species together account for less than 4% of the TOC in
374 aqSOA (Table 1). Note that the importance of organic acids is likely underestimated as IC only
375 quantifies a limited number of low molecular weight aliphatic acids. Nano-DESI analysis further
376 reveals the presence of a number of aromatic compounds with substituted carboxyl groups (e.g.,
377 aromatic esters; Fig. S10) and the formation of highly oxygenated C3-C5 aliphatic species in all
378 samples, some of which (e.g., $C_3H_4O_4$, $C_4H_6O_4$ and $C_5H_6O_5$) are likely carboxylic acids based on
379 DBE values. Furthermore, both nano-DESI and AMS analyses identify demethoxylated aromatic
380 products (e.g., $C_{15}H_{16}O_6$ and $C_{15}H_{16}O_9$ in Table 2). These results together indicate that various
381 fragmentation pathways, such as the cleavage of the aromatic rings and the losses of methoxy (-
382 | OCH₃) groups, are also important during the aqueous-phase reactions of phenols.

383 Based on these results, we propose a scheme in Fig. 7 of the main pathways of aqSOA
384 formation through the reactions of phenols + $^3\text{C}^*$. Briefly, phenols react with $^3\text{C}^*$ and undergo
385 multiple steps to ~~eventually~~ form HOOH (Anastasio et al., 1997), which is a source of $\bullet\text{OH}$ via
386 photolysis. The addition of $\bullet\text{OH}$ to the aromatic ring, followed by O_2 addition and $\text{HO}_2\bullet$
387 elimination, ~~lead~~leads to the formation of hydroxylated products (Barzaghi and Herrmann, 2002).
388 In the meantime, the $\bullet\text{OH}$ -phenol adduct can undergo unimolecular elimination of H_2O to form a
389 phenoxy radical (Atkinson et al., 1992; Barzaghi and Herrmann, 2002; Olariu et al., 2002),
390 which then combines with another radical to form dimer and higher oligomers. Note that the
391 amount of HOOH produced in the reactions of phenols + $^3\text{C}^*$ is small and $\bullet\text{OH}$ oxidation appears
392 to be negligible compared to the oxidation of phenols by $^3\text{C}^*$ (Smith et al., 2014). Phenoxy
393 radical may also form from the oxidation of phenols by $^3\text{C}^*$ via electron transfer coupled with
394 proton transfer from the phenoxyl radical cation or from solvent water (Anastasio et al., 1997).
395 Demethoxylation takes place through attachment of $\bullet\text{OH}$ to ring positions occupied by methoxyl
396 groups, followed by elimination of a methanol molecule to form semiquinone radicals (Steenken
397 and O'Neill, 1977). Esterification of phenols ~~can occur as a result of~~occurs through the reactions
398 with organic acids (Offenhauer, 1964). Furthermore, the reactants and the products from all these
399 pathways may undergo ring-opening process, forming ketones and carboxylic acids. Similar
400 species, including oligomers, esters, carbonyls, carboxylic acids, and demethoxylated products,
401 can be formed in $\bullet\text{OH}$ -mediated reactions as well (Sun et al., 2010), although apparently with
402 different reaction yields and rates.

403 ***3.3 Comparisons of phenolic aqSOA produced from different oxidants: $\bullet\text{OH}$ vs. $^3\text{C}^*$***

404 As discussed above, aqueous reactions of phenols produce a variety of low-volatility
405 species including oligomers, functionalized monomer and oligomers (with varying numbers of

406 carbonyl, carboxyl, ester, and hydroxyl groups), and small organic acids (e.g., formate, acetate,
407 oxalate, and malate). Although aqSOA formed from the same precursor generally appear to be
408 chemically similar, there are significant compositional differences between the products from
409 •OH and ³C* reactions. Overall, the molecular compositions of guaiacol and phenol aqSOA are
410 more dependent on the oxidant than are syringol aqSOA (Fig. 5). Similarly, the AMS spectral
411 patterns at $m/z \geq 80$ exhibit more significant differences between •OH and ³C* for guaiacol ($r^2 =$
412 0.65; Fig. 2j) and phenol ($r^2 = 0.42$; Fig. 2l) whereas those for syringol are almost identical ($r^2 =$
413 0.97; Fig. 2h). Furthermore, a majority of the aqSOA molecules of phenol + •OH contain only
414 one benzene ring, whereas the ³C* reaction produces more oligomers and substituted species
415 based on the DBE values.

416 ~~Since the AMS results are quantitative, we further compare the relative abundances of~~
417 ~~signature ions in the AMS spectra of different aqSOA (Fig. 8). Since the fragmentation pattern from~~
418 ~~70 eV electron ionization is reproducible (McLafferty and Turecek, 1993), unique ions can be~~
419 ~~used as tracer species to quantify the concentration of the parent compound. Thus, we further~~
420 ~~compare the relative abundances of signature ions in the AMS spectra of the aqSOA formed~~
421 ~~from •OH- and ³C*-mediated reactions (Fig. 8). Details on the signature ions and their proposed~~
422 precursors are given in Table S1. All these ions are odd electron ions, which usually have special
423 mechanistic significances and are more indicative of the chemical identities of the precursors
424 (McLafferty and Turecek, 1993). These ions can potentially be used to analyze ambient organic
425 aerosol data for the presence of phenolic aqSOA. For instance, a previous study by our group
426 observed $C_{16}H_{18}O_6^+$ (m/z 306) and $C_{14}H_{14}O_4^+$ (m/z 246) – signature ions representing syringol
427 and guaiacol dimers, respectively, in ambient aerosols significantly influenced by wood
428 combustion and fog processing (Sun et al., 2010). Similar to the nano-DESI results, the AMS

429 results also indicate that the aqSOA formed via $^3\text{C}^*$ are more enriched of dimers and higher
430 oligomers compared to $\bullet\text{OH}$ for a given phenol. These observations suggest that more coupling
431 of phenoxy radicals takes place during reactions initiated by $^3\text{C}^*$ than by $\bullet\text{OH}$. On the other hand,
432 both IC and nano-DESI results indicate that $\bullet\text{OH}$ -mediated reactions promote the formation of
433 organic acids and other ~~small~~-ring-opening species ($n_c < 6$) (see Sect. 3.2), consistent with the
434 observations that $\bullet\text{OH}$ reaction generally leads to more oxidized aqSOA as well as water-soluble
435 volatile species (Table 1).

436 A possible reason for the compositional differences observed in the aqSOA of the same
437 precursor but different oxidants is that $^3\text{C}^*$ reacts faster with phenols (Smith et al., 2014) and
438 thus takes shorter time to oxidize the same amount of phenols compared to $\bullet\text{OH}$. Longer
439 illumination allows further oxidation and fragmentation of higher molecular weight species to
440 happen, leading to the formation of smaller molecules with fewer aromatic rings. Indeed, the
441 compositions of syringol aqSOA, which were produced after comparable illumination durations,
442 are highly similar between the two oxidation conditions according to both nano-DESI and AMS
443 results whereas the difference is the largest for phenol aqSOA whose illumination times are
444 substantially different between $^3\text{C}^*$ and $\bullet\text{OH}$ oxidation (Figs. 2 and 5). However, the fact that
445 there are more oligomers and their derivatives in guaiacol + $^3\text{C}^*$ condition compared to syringol
446 + $\bullet\text{OH}$ (Fig. 5) even though the ~~guaiacol solution was illuminated longer~~illumination durations
447 are similar (Table 1) suggests that coupling of phenoxy radicals is a more favored pathway
448 through $^3\text{C}^*$ reaction.

449 ***3.4 Volatility profiles and UV-vis absorption spectra of phenolic aqSOA***

450 As discussed above, the chemical compositions of ~~the~~ phenolic aqSOA are complex. As a
451 result, the volatilities of the aqSOA species span a broad range, from very low vapor pressure

452 compounds such as oligomers to more volatile species such as low molecular weight acids.
453 Figure 9 shows the volatility profiles of phenolic aqSOA formed from $^3\text{C}^*$ reactions measured by
454 a thermodenuder coupled with the AMS. Ammonium sulfate and ammonium nitrate were
455 analyzed simultaneously as references. On average, phenolic aqSOA are more volatile than
456 ammonium sulfate, but less volatile than ammonium nitrate (Fig. 9). The fact that a significant
457 fraction of the aqSOA mass remains in the particle phase even at 200 °C (Fig. 9) is consistent
458 with the presence of some very low volatility species such as oligomers. Compared to guaiacol
459 and syringol aqSOA, phenol aqSOA show the slowest decay with increasing TD temperature,
460 indicating that they are comprised of more low-volatility species. This is consistent with our
461 chemical analyses which reveal that the aqSOA of phenol + $^3\text{C}^*$ are composed of a larger
462 fraction of species containing more than two aromatic rings, including trimer and higher
463 oligomers (Fig. 5) ~~and~~. This is also consistent with fact that the O/C ratios of phenol aqSOA are
464 ~~also~~ highest among all three precursors for the same oxidant. These results together suggest that
465 the volatility of phenolic aqSOA is strongly influenced by both polymer contents and average
466 oxidation degree, as reported previously (Huffman et al., 2009).

467 Recently, light-absorbing OA, also termed ~~as~~ “brown carbon”, has attracted much
468 attention, due to their ability to absorb sunlight and thus affect the radiative budget of the earth
469 (Shapiro et al., 2009). Previous studies have shown that the aqueous-phase oxidation of phenols
470 forms low-volatility oligomers, which absorb significant amounts of UV-visible light and likely
471 account for a significant portion of atmospheric HULIS (Gelencser et al., 2003; Chang and
472 Thompson, 2010). In this study, we examined the optical properties of phenolic aqSOA using
473 UV-vis spectroscopy. Figure 10 shows an example of the UV-vis spectra of syringol aqSOA
474 formed in the reactions with $^3\text{C}^*$ and $\bullet\text{OH}$, respectively, at $t_{1/2}$. Both syringol aqSOA samples

475 absorb in the tropospheric sunlight wavelengths (> 300 nm), while syringol does not. This
476 enhancement is likely explained by the formation of conjugated structures as a result of
477 polymerization and functionalization due to the additions of hydroxyl, carbonyl, and carboxyl
478 functional groups to the aromatic rings. [Phenol and guaiacol aqSOA also show enhanced](#)
479 [absorption in the tropospheric sunlight wavelengths \(\$> 300\$ nm\), while phenol and guaiacol](#)
480 [themselves do not.](#) These results indicate that aqueous-phase reactions of phenols are likely an
481 important source of brown carbon in the atmosphere, especially in regions influenced by biomass
482 burning.

483 **4. Conclusions and implications**

484 We thoroughly characterized the chemical composition and studied the volatility and
485 optical properties of phenolic aqSOA formed via reactions with two different oxidants: $^3\text{C}^*$ and
486 $\bullet\text{OH}$. Elemental analysis of the AMS spectra indicates that all phenolic aqSOA are highly
487 oxidized (O/C ratios: 0.85-1.23), despite the fact that some of the reactions were very fast ($t_{1/2} <$
488 1 hr for syringol). For the same oxidant, the oxidation degree of the aqSOA formed at $t_{1/2}$ follows
489 the order: phenol $>$ guaiacol $>$ syringol. A large number of aqSOA molecules are identified,
490 including oligomers (up to hexamers) and their derivatives with varying numbers of carbonyl,
491 carboxyl, ester, and hydroxyl groups. A large number of ring-opening species ($n_c < 6$) including
492 small organic acids (e.g., oxalate, formate, and acetate) are also identified. While the bulk
493 compositions of the aqSOA are overall similar at $t_{1/2}$ between the two oxidants for a given
494 precursor, compositional differences are observed. Generally speaking, reactions mediated by
495 $\bullet\text{OH}$ produce more highly oxygenated species with a single aromatic ring, while oxidation by
496 $^3\text{C}^*$ enhances the formation of higher molecular weight species including oligomers and their
497 oxygenated derivatives. The physical properties, such as volatility and light absorptivity, of the

498 phenol aqSOA depend on their chemical compositions. Our thermodenuder experiments indicate
499 that the volatility profiles of phenolic aqSOA are influenced by both oligomer contents and
500 average oxidation degree. In addition, the formation of aqSOA species with enhanced conjugated
501 double bonds is probably responsible for the significant light absorption in the actinic region,
502 suggesting that aqueous-phase reactions of phenols are an important source of brown carbon in
503 the atmosphere.

504 Overall, our results indicate that aqueous-phase processing of phenols represents an
505 important pathway for the production of low-volatility, highly oxygenated and high molecular
506 weight species, which remain in the particle phase after water evaporation. Since ~~aqSOA formed~~
507 ~~from reactions of~~ phenolic ~~compounds are~~ aqSOA is both water soluble and light absorbing,
508 ~~understanding the impacts of~~ these reactions ~~might significantly influence~~ on the chemical and
509 physical properties, and thus the climatic and health effects, of atmospheric particles ~~may be~~
510 ~~important, especially~~ in regions influenced by biomass burning emissions. ~~In this study, we also~~
511 ~~identified a number of~~ An approach for evaluating the importance of phenolic aqSOA formation
512 in the atmosphere is to systematically analyze the AMS mass spectra of ambient aerosol for
513 signature ions ~~that are~~ representative of phenolic aqSOA, ~~e.g.,~~ $C_{16}H_{18}O_6^+$ ($m/z = 306$) for
514 syringol dimer, $C_{14}H_{14}O_4^+$ ($m/z = 246$) for guaiacol dimer, $C_{14}H_{14}O_5^+$ ($m/z = 262$) and $C_{14}H_{14}O_6^+$
515 ($m/z = 278$) for hydroxylated guaiacol dimer, $C_{12}H_{10}O_2^+$ ($m/z = 186$) for phenol dimer, $C_{21}H_{20}O_6^+$
516 ($m/z = 368$) for guaiacol trimer, and $C_{18}H_{14}O_3^+$ ($m/z = 278$) for phenol trimer (Fig. 8). AMS has
517 been broadly applied for chemical analysis of ambient aerosol and multivariate statistical
518 approaches (e.g., positive matrix factorization) have been frequently used on organic aerosol
519 mass spectral data to determine factors representing different sources and processes (Ulbrich et
520 al., 2009; Zhang et al., 2011). An important criterion for validating the extracted factor is via

521 examining the mass spectra of the factors for signature ions (Zhang et al., 2011). ~~The signature~~
522 ~~ions identified in this study could be compared to ambient organic aerosol mass spectrometry~~
523 ~~data to investigate the impacts of phenolic aqSOA formation.~~ The fact that AMS uses 70 eV EI
524 ionization, which ionizes and fragments molecules with reproducible pattern (McLafferty and
525 Turecek, 1993), allows for the identification and quantification of certain compounds or
526 compound classes in a mixture via signature ions. Indeed, previous studies have demonstrated
527 the capability of using unique AMS ions to fingerprint species such as hydrocarbon-like and
528 oxygenated organic aerosols (Zhang et al., 2005), polycyclic aromatic hydrocarbons (PAH)
529 (Dzepina et al., 2007), methanesulfonic acid (MSA) (Ge et al., 2012), and certain nitrogen- and
530 sulfur-containing organic aerosols (Farmer et al., 2010; Ge et al., 2014).

531 With this in mind, this study suggests several ions that are potentially representative of
532 phenolic aqSOA, including $C_{16}H_{18}O_6^+$ ($m/z = 306$) for syringol dimer, $C_{14}H_{14}O_4^+$ ($m/z = 246$) for
533 guaiacol dimer, $C_{14}H_{14}O_5^+$ ($m/z = 262$) and $C_{14}H_{14}O_6^+$ ($m/z = 278$) for hydroxylated guaiacol
534 dimer, $C_{12}H_{10}O_2^+$ ($m/z = 186$) for phenol dimer, $C_{21}H_{20}O_6^+$ ($m/z = 368$) for guaiacol trimer, and
535 $C_{18}H_{14}O_3^+$ ($m/z = 278$) for phenol trimer (Fig. 8). Since all these ions have odd number of
536 electrons with relatively high m/z 's, their productions in the AMS are more directly linked to the
537 specific parent compounds, meaning that they are less likely contributed by confounding
538 molecules (McLafferty and Turecek, 1993). In addition, while large hydrocarbon molecules, e.g.,
539 those from vehicle emissions, may generate significant ion signals at $m/z > 200$, most of them are
540 even-electron ions and contain no oxygen. They are therefore easily differentiated from the
541 isobaric ions from phenolic SOA. Nevertheless, it is important to point out that the validity of
542 using the aqSOA signature ions identified in this study needs to be evaluated by examining
543 ambient organic aerosol mass spectrometry data. In addition, analyzing field samples with nano-

544 | [DESI may also provide important insights into the impacts of aqueous phase processing of](#)
545 | [phenolic compounds in the atmosphere.](#)

546 | **Acknowledgements**

547 | This work was supported by the U.S. National Science Foundation, Grant No. AGS-
548 | 1036675, [and](#) the California Agricultural Experiment Station (Projects CA-D-ETX-2102-H and
549 | CA-D*-LAW-6403-RR). The nano-DESI ~~measurements were~~[MS analysis was](#) performed at the
550 | W.R. Wiley Environmental Molecular Sciences Laboratory (EMSL) - a national scientific user
551 | facility located at PNNL, and sponsored by the Office of Biological and Environmental Research
552 | of the U.S. PNNL is operated for US DOE by Battelle Memorial Institute under Contract No.
553 | DE-AC06-76RL0 1830. Additional funding was provided by a Jastro-Shields Graduate Research
554 | Award (UC Davis) and ~~a~~ graduate [fellowship](#)~~fellowships~~ from the Atmospheric Aerosols and
555 | Health (AAH) program at UC Davis to Lu Yu [and Jeremy Smith](#). We thank Dr. Ann Dillner,
556 | Kathryn George, and Dr. Sonya Collier for help with experiments.

557 | **References**

558 | Aiken, A. C., Decarlo, P. F., Kroll, J. H., Worsnop, D. R., Huffman, J. A., Docherty, K. S.,
559 | Ulbrich, I. M., Mohr, C., Kimmel, J. R., Sueper, D., Sun, Y., Zhang, Q., Trimborn, A., Northway, M.,
560 | Ziemann, P. J., Canagaratna, M. R., Onasch, T. B., Alfarra, M. R., Prevot, A. S. H., Dommen, J.,
561 | Duplissy, J., Metzger, A., Baltensperger, U. and Jimenez, J. L.: O/C and OM/OC ratios of primary,
562 | secondary, and ambient organic aerosols with high-resolution time-of-flight aerosol mass spectrometry,
563 | Environ. Sci. Technol., 42, 4478-4485, doi:10.1021/es703009q, 2008.

564 | Allan, J. D., Delia, A. E., Coe, H., Bower, K. N., Alfarra, M. R., Jimenez, J. L., Middlebrook, A.
565 | M., Drewnick, F., Onasch, T. B., Canagaratna, M. R., Jayne, J. T. and Worsnop, D. R.: A generalised
566 | method for the extraction of chemically resolved mass spectra from Aerodyne aerosol mass spectrometer
567 | data, J. Aerosol Sci., 35, 909-922, doi:10.1016/j.jaerosci.2004.02.007, 2004.

568 | Altieri, K. E., Carlton, A. G., Lim, H. J., Turpin, B. J. and Seitzinger, S. P.: Evidence for
569 | oligomer formation in clouds: reactions of isoprene oxidation products, Environ. Sci. Technol., 40, 4956-
570 | 4960, doi:10.1021/es052170n, 2006.

571 | Anastasio, C., Faust, B. C. and Rao, C. J.: Aromatic carbonyl compounds as aqueous-phase
572 | photochemical sources of hydrogen peroxide in acidic sulfate aerosols, fogs, and clouds .1. Non-phenolic
573 | methoxybenzaldehydes and methoxyacetophenones with reductants (phenols), Environ. Sci. Technol., 31,
574 | 218-232, doi:10.1021/es960359g, 1997.

575 | Anastasio, C. and McGregor, K. G.: Chemistry of fog waters in California's Central Valley: 1. In
576 | situ photoformation of hydroxyl radical and singlet molecular oxygen, Atmos. Environ., 35, 1079-1089,
577 | doi:10.1016/s1352-2310(00)00281-8, 2001.

578 Arakaki, T., Anastasio, C., Kuroki, Y., Nakajima, H., Okada, K., Kotani, Y., Handa, D., Azechi,
579 S., Kimura, T., Tsuchi, A. and Miyagi, Y.: A General Scavenging Rate Constant for Reaction of
580 Hydroxyl Radical with Organic Carbon in Atmospheric Waters, *Environ. Sci. Technol.*, 47, 8196-8203,
581 doi:10.1021/es401927b, 2013.

582 Aregahegn, K. Z., Noziere, B. and George, C.: Organic aerosol formation photo-enhanced by the
583 formation of secondary photosensitizers in aerosols, *Faraday Disc.*, 165, 123-134,
584 doi:10.1039/C3FD00044C, 2013.

585 Atkinson, R., Aschmann, S. M. and Arey, J.: Reactions of hydroxyl and nitrogen trioxide radicals
586 with phenol, cresols, and 2-nitrophenol at 296±2 K, *Environ. Sci. Technol.*, 26, 1397-1403,
587 doi:10.1021/es00031a018, 1992.

588 Barzagli, P. and Herrmann, H.: A mechanistic study of the oxidation of phenol by OH/NO₂/NO₃
589 in aqueous solution, *Phys. Chem. Chem. Phys.*, 4, 3669-3675, doi:10.1039/b201652d, 2002.

590 Bateman, A. P., Laskin, J., Laskin, A. and Nizkorodov, S. A.: Applications of high-resolution
591 electrospray ionization mass spectrometry to measurements of average oxygen to carbon ratios in
592 secondary organic aerosols, *Environ. Sci. Technol.*, 46, 8315-8324, doi:10.1021/es3017254, 2012.

593 Blando, J. D. and Turpin, B. J.: Secondary organic aerosol formation in cloud and fog droplets: a
594 literature evaluation of plausibility, *Atmos. Environ.*, 34, 1623-1632, doi:10.1016/S1352-2310(99)00392-
595 1, 2000.

596 Canagaratna, M. R., Jayne, J. T., Jimenez, J. L., Allan, J. D., Alfarra, M. R., Zhang, Q., Onasch, T.
597 B., Drewnick, F., Coe, H., Middlebrook, A., Delia, A., Williams, L. R., Trimborn, A. M., Northway, M. J.,
598 DeCarlo, P. F., Kolb, C. E., Davidovits, P. and Worsnop, D. R.: Chemical and microphysical
599 characterization of ambient aerosols with the aerodyne aerosol mass spectrometer, *Mass Spectrom. Rev.*,
600 26, 185-222, doi:10.1002/mas.20115, 2007.

601 Canonica, S., Hellrung, B. and Wirz, J.: Oxidation of phenols by triplet aromatic ketones in
602 aqueous solution, *J. Phys. Chem. A*, 104, 1226-1232, doi:10.1021/jp9930550, 2000.

603 Chang, J. L. and Thompson, J. E.: Characterization of colored products formed during irradiation
604 of aqueous solutions containing H₂O₂ and phenolic compounds, *Atmos. Environ.*, 44, 541-551,
605 doi:10.1016/j.atmosenv.2009.10.042, 2010.

606 Chhabra, P. S., Ng, N. L., Canagaratna, M. R., Corrigan, A. L., Russell, L. M., Worsnop, D. R.,
607 Flagan, R. C. and Seinfeld, J. H.: Elemental composition and oxidation of chamber organic aerosol,
608 *Atmos. Chem. Phys.*, 11, 8827-8845, doi:10.5194/acp-11-8827-2011, 2011.

609 Collier, S. and Zhang, Q.: Gas-phase CO₂ subtraction for improved measurements of the organic
610 aerosol mass concentration and oxidation degree by an aerosol mass spectrometer, *Environ. Sci. Technol.*,
611 47, 14324-14331, doi:10.1021/es404024h, 2013.

612 DeCarlo, P. F., Kimmel, J. R., Trimborn, A., Northway, M. J., Jayne, J. T., Aiken, A. C., Gonin,
613 M., Fuhrer, K., Horvath, T., Docherty, K. S., Worsnop, D. R. and Jimenez, J. L.: Field-deployable, high-
614 resolution, time-of-flight aerosol mass spectrometer, *Anal. Chem.*, 78, 8281-8289,
615 doi:10.1021/ac061249n, 2006.

616 Dzepina, K., Arey, J., Marr, L. C., Worsnop, D. R., Salcedo, D., Zhang, Q., Onasch, T. B.,
617 Molina, L. T., Molina, M. J. and Jimenez, J. L.: Detection of particle-phase polycyclic aromatic
618 hydrocarbons in Mexico City using an aerosol mass spectrometer, *Int. J. Mass Spectrom.*, 263, 152-170,
619 doi:10.1016/j.ijms.2007.01.010, 2007.

620 Ervens, B., Turpin, B. J. and Weber, R. J.: Secondary organic aerosol formation in cloud droplets
621 and aqueous particles (aqSOA): a review of laboratory, field and model studies, *Atmos. Chem. Phys.*, 11,
622 11069-11102, doi:10.5194/acp-11-11069-2011, 2011.

623 Farmer, D. K., Matsunaga, A., Docherty, K. S., Surratt, J. D., Seinfeld, J. H., Ziemann, P. J. and
624 Jimenez, J. L.: Response of an aerosol mass spectrometer to organonitrates and organosulfates and
625 implications for atmospheric chemistry, *Proc. Natl. Acad. Sci.*, 107, 6670-6675,
626 doi:10.1073/pnas.0912340107, 2010.

627 Fierz, M., Vernooij, M. G. C. and Burtscher, H.: An improved low-flow thermodenuder, *J.*
628 *Aerosol Sci.*, 38, 1163-1168, doi:10.1016/j.jaerosci.2007.08.006, 2007.

629 Ge, X., Setyan, A., Sun, Y. and Zhang, Q.: Primary and secondary organic aerosols in Fresno,
630 California during wintertime: Results from high resolution aerosol mass spectrometry, *J. Geophys. Res.*,
631 117, D19301, doi:10.1029/2012JD018026, 2012.

632 Ge, X., Shaw, S. L. and Zhang, Q.: Toward understanding amines and their degradation products
633 from postcombustion CO₂ capture processes with aerosol mass spectrometry, *Environ. Sci. Technol.*, 48,
634 5066-5075, doi:10.1021/es4056966, 2014.

635 Gelencser, A., Hoffer, A., Kiss, G., Tombacz, E., Kurdi, R. and Bencze, L.: In-situ formation of
636 light-absorbing organic matter in cloud water, *J. Atmos. Chem.*, 45, 25-33, doi:10.1023/a:1024060428172,
637 2003.

638 George, K. M., Ruthenburg, T. C., Smith, J. D., Anastasio, C., Yu, L., Zhang, Q. and Dillner, A.:
639 FT-IR quantification of the carbonyl functional group in aqueous-phase secondary organic aerosol from
640 phenols, *Atmos. Environ.*, 2014.

641 Hallquist, M., Wenger, J. C., Baltensperger, U., Rudich, Y., Simpson, D., Claeys, M., Dommen,
642 J., Donahue, N. M., George, C., Goldstein, A. H., Hamilton, J. F., Herrmann, H., Hoffmann, T., Iinuma,
643 Y., Jang, M., Jenkin, M. E., Jimenez, J. L., Kiendler-Scharr, A., Maenhaut, W., McFiggans, G., Mentel, T.
644 F., Monod, A., Prevot, A. S. H., Seinfeld, J. H., Surratt, J. D., Szmigielski, R. and Wildt, J.: The
645 formation, properties and impact of secondary organic aerosol: current and emerging issues, *Atmos.*
646 *Chem. Phys.*, 9, 5155-5236, doi:10.5194/acp-9-5155-2009, 2009.

647 Hawthorne, S. B., Krieger, M. S., Miller, D. J. and Mathiason, M. B.: Collection and quantitation
648 of methoxylated phenol tracers for atmospheric-pollution from residential wood stoves, *Environ. Sci.*
649 *Technol.*, 23, 470-475, doi:10.1021/es00181a013, 1989.

650 Hawthorne, S. B., Miller, D. J., Langenfeld, J. J. and Krieger, M. S.: PM-10 high-volume
651 collection and quantitation of semi- and nonvolatile phenols, methoxylated phenols, alkanes, and
652 polycyclic aromatic hydrocarbons from winter urban air and their relationship to wood smoke emissions,
653 *Environ. Sci. Technol.*, 26, 2251-2262, doi:10.1021/es00035a026, 1992.

654 Huffman, J. A., Docherty, K. S., Mohr, C., Cubison, M. J., Ulbrich, I. M., Ziemann, P. J., Onasch,
655 T. B. and Jimenez, J. L.: Chemically-resolved volatility measurements of organic aerosol from different
656 sources, *Environ. Sci. Technol.*, 43, 5351-5357, doi:10.1021/es803539d, 2009.

657 Hughey, C. A., Hendrickson, C. L., Rodgers, R. P., Marshall, A. G. and Qian, K. N.: Kendrick
658 mass defect spectrum: A compact visual analysis for ultrahigh-resolution broadband mass spectra, *Anal.*
659 *Chem.*, 73, 4676-4681, doi:10.1021/ac010560w, 2001.

660 Jaitly, N., Mayampurath, A., Littlefield, K., Adkins, J. N., Anderson, G. A. and Smith, R. D.:
661 Decon2LS: An open-source software package for automated processing and visualization of high
662 resolution mass spectrometry data, *BMC Bioinformatics*, 10, 87, doi:10.1186/1471-2105-10-87, 2009.

663 Jimenez, J. L., Canagaratna, M. R., Donahue, N. M., Prevot, A. S. H., Zhang, Q., Kroll, J. H.,
664 DeCarlo, P. F., Allan, J. D., Coe, H., Ng, N. L., Aiken, A. C., Docherty, K. S., Ulbrich, I. M., Grieshop, A.
665 P., Robinson, A. L., Duplissy, J., Smith, J. D., Wilson, K. R., Lanz, V. A., Hueglin, C., Sun, Y. L., Tian,
666 J., Laaksonen, A., Raatikainen, T., Rautiainen, J., Vaattovaara, P., Ehn, M., Kulmala, M., Tomlinson, J.
667 M., Collins, D. R., Cubison, M. J., Dunlea, E. J., Huffman, J. A., Onasch, T. B., Alfarra, M. R., Williams,
668 P. I., Bower, K., Kondo, Y., Schneider, J., Drewnick, F., Borrmann, S., Weimer, S., Demerjian, K.,
669 Salcedo, D., Cottrell, L., Griffin, R., Takami, A., Miyoshi, T., Hatakeyama, S., Shimono, A., Sun, J. Y.,
670 Zhang, Y. M., Dzepina, K., Kimmel, J. R., Sueper, D., Jayne, J. T., Herndon, S. C., Trimborn, A. M.,
671 Williams, L. R., Wood, E. C., Middlebrook, A. M., Kolb, C. E., Baltensperger, U. and Worsnop, D. R.:
672 Evolution of organic aerosols in the atmosphere, *Science*, 326, 1525-1529, doi:10.1126/science.1180353,
673 2009.

674 Kanakidou, M., Seinfeld, J. H., Pandis, S. N., Barnes, I., Dentener, F. J., Facchini, M. C., Van
675 Dingenen, R., Ervens, B., Nenes, A., Nielsen, C. J., Swietlicki, E., Putaud, J. P., Balkanski, Y., Fuzzi, S.,
676 Horth, J., Moortgat, G. K., Winterhalter, R., Myhre, C. E. L., Tsigaridis, K., Vignati, E., Stephanou, E. G.
677 and Wilson, J.: Organic aerosol and global climate modelling: a review, *Atmos. Chem. Phys.*, 5, 1053-
678 1123, doi:10.5194/acp-5-1053-2005, 2005.

679 Krueve, A., Kaupmees, K., Liigand, J. and Leito, I.: Negative Electrospray Ionization via
680 Deprotonation: Predicting the Ionization Efficiency, *Anal Chem*, 86, 4822-4830, doi:10.1021/ac404066v,
681 2014.

682 Leuenberger, C., Ligocki, M. P. and Pankow, J. F.: Trace organic compounds in rain. 4. Identities,
683 concentrations, and scavenging mechanisms for phenols in urban air and rain, *Environ. Sci. Technol.*, 19,
684 1053-1058, doi:10.1021/es00141a005, 1985.

685 Lim, H. J., Carlton, A. G. and Turpin, B. J.: Isoprene forms secondary organic aerosol through
686 cloud processing: Model simulations, *Environ. Sci. Technol.*, 39, 4441-4446, doi:10.1021/es048039h,
687 2005.

688 McLafferty, F. W. and Turecek, F.: *Interpretation of Mass Spectra*, University Science Books,
689 Mill Valley, California, 1993.

690 Monge, M. E., Rosenørn, T., Favez, O., Müller, M., Adler, G., Abo Riziq, A., Rudich, Y.,
691 Herrmann, H., George, C. and D'Anna, B.: Alternative pathway for atmospheric particles growth, *Proc.*
692 *Natl. Acad. Sci.*, 109, 6840-6844, doi:10.1073/pnas.1120593109, 2012.

693 Murphy, D. M., Cziczo, D. J., Froyd, K. D., Hudson, P. K., Matthew, B. M., Middlebrook, A. M.,
694 Peltier, R. E., Sullivan, A., Thomson, D. S. and Weber, R. J.: Single-particle mass spectrometry of
695 tropospheric aerosol particles, *J. Geophys. Res.-Atmos.*, 111, D23S32, doi:10.1029/2006jd007340, 2006.

696 Offenhauer, R. D.: The direct esterification of phenols, *J. Chem. Educ.*, 41, 39,
697 doi:10.1021/ed041p39, 1964.

698 Ofner, J., Krüger, H. U., Grothe, H., Schmitt-Kopplin, P., Whitmore, K. and Zetzsch, C.:
699 Physico-chemical characterization of SOA derived from catechol and guaiacol - a model substance for the
700 aromatic fraction of atmospheric HULIS, *Atmos. Chem. Phys.*, 11, 1-15, doi:10.5194/acp-11-1-2011,
701 2011.

702 Olariu, R. I., Klotz, B., Barnes, I., Becker, K. H. and Mocanu, R.: FT-IR study of the ring-
703 retaining products from the reaction of OH radicals with phenol, o-, m-, and p-cresol, *Atmos. Environ.*, 36,
704 3685-3697, doi:10.1016/s1352-2310(02)00202-9, 2002.

705 Pellegrin, V.: Molecular formulas of organic compounds: the nitrogen rule and degree of
706 unsaturation, *J. Chem. Educ.*, 60, 626-633, doi:10.1021/ed060p626, 1983.

707 Roach, P. J., Laskin, J. and Laskin, A.: Molecular characterization of organic aerosols using
708 nanospray-desorption/electrospray ionization-mass spectrometry, *Anal. Chem.*, 82, 7979-7986,
709 doi:10.1021/ac101449p, 2010a.

710 Roach, P. J., Laskin, J. and Laskin, A.: Nanospray desorption electrospray ionization: an ambient
711 method for liquid-extraction surface sampling in mass spectrometry, *Analyst*, 135, 2233-2236,
712 doi:10.1039/c0an00312c, 2010b.

713 Roach, P. J., Laskin, J. and Laskin, A.: Higher-order mass defect analysis for mass spectra of
714 complex organic mixtures, *Anal. Chem.*, 83, 4924-4929, doi:10.1021/ac200654j, 2011.

715 Rossignol, S., Aregahegn, K. Z., Tinel, L., Fine, L., Noziere, B. and George, C.: Glyoxal Induced
716 Atmospheric Photosensitized Chemistry Leading to Organic Aerosol Growth, *Environ. Sci. Technol.*, 48,
717 3218-3227, doi:10.1021/es405581g, 2014.

718 Sagebiel, J. C. and Seiber, J. N.: Studies on the occurrence and distribution of wood smoke
719 marker compounds in foggy atmospheres, *Environ. Toxicol. Chem.*, 12, 813-822,
720 doi:10.1002/etc.5620120504, 1993.

721 Sander, R.: Compilation of Henry's Law constants for inorganic and organic species of potential
722 importance in environmental chemistry, available at: <http://irs.ub.rug.nl/dbi/4581696d8b3ed> (last access:
723 14 December 2006), 1999.

724 Schauer, J. J., Kleeman, M. J., Cass, G. R. and Simoneit, B. R. T.: Measurement of emissions
725 from air pollution sources. 3. C-1-C-29 organic compounds from fireplace combustion of wood, *Environ.*
726 *Sci. Technol.*, 35, 1716-1728, doi:10.1021/es001331e, 2001.

727 Shapiro, E. L., Szprengiel, J., Sareen, N., Jen, C. N., Giordano, M. R. and McNeill, V. F.: Light-
728 absorbing secondary organic material formed by glyoxal in aqueous aerosol mimics, *Atmos. Chem. Phys.*,
729 9, 2289-2300, doi:10.5194/acp-9-2289-2009, 2009.

730 Simoneit, B. R. T., Schauer, J. J., Nolte, C. G., Oros, D. R., Elias, V. O., Fraser, M. P., Rogge, W.
731 F. and Cass, G. R.: Levoglucosan, a tracer for cellulose in biomass burning and atmospheric particles,
732 *Atmos. Environ.*, 33, 173-182, doi:10.1016/s1352-2310(98)00145-9, 1999.

733 Smith, J. D., Sio, V., Yu, L., Zhang, Q. and Anastasio, C.: Secondary organic aerosol production
734 from aqueous reactions of atmospheric phenols with an organic triplet excited state, *Environ. Sci.*
735 *Technol.*, 48, 1049-1057, doi:10.1021/es4045715, 2014.

736 Steenken, S. and O'Neill, P.: Oxidative demethoxylation of methoxylated phenols and
737 hydroxybenzoic acids by the hydroxyl radical. An in situ electron spin resonance, conductometric pulse
738 radiolysis and product analysis study, *J. Phys. Chem.*, 81, 505-508, doi:10.1021/j100521a002, 1977.

739 Sun, Y., Zhang, Q., Macdonald, A. M., Hayden, K., Li, S. M., Liggio, J., Liu, P. S. K., Anlauf, K.
740 G., Leaitch, W. R., Steffen, A., Cubison, M., Worsnop, D. R., van Donkelaar, A. and Martin, R. V.: Size-
741 resolved aerosol chemistry on Whistler Mountain, Canada with a high-resolution aerosol mass
742 spectrometer during INTEX-B, *Atmos. Chem. Phys.*, 9, 3095-3111, doi:10.5194/acp-9-3095-2009, 2009.

743 Sun, Y. L., Zhang, Q., Anastasio, C. and Sun, J.: Insights into secondary organic aerosol formed
744 via aqueous-phase reactions of phenolic compounds based on high resolution mass spectrometry, *Atmos.*
745 *Chem. Phys.*, 10, 4809-4822, doi:10.5194/acp-10-4809-2010, 2010.

746 Ulbrich, I. M., Canagaratna, M. R., Zhang, Q., Worsnop, D. R. and Jimenez, J. L.: Interpretation
747 of organic components from Positive Matrix Factorization of aerosol mass spectrometric data, *Atmos.*
748 *Chem. Phys.*, 9, 2891-2918, doi:10.5194/acp-9-2891-2009, 2009.

749 Yee, L. D., Kautzman, K. E., Loza, C. L., Schilling, K. A., Coggon, M. M., Chhabra, P. S., Chan,
750 M. N., Chan, A. W. H., Hersey, S. P., Crounse, J. D., Wennberg, P. O., Flagan, R. C. and Seinfeld, J. H.:
751 Secondary organic aerosol formation from biomass burning intermediates: phenol and methoxyphenols,
752 *Atmos. Chem. Phys.*, 13, 8019-8043, doi:10.5194/acp-13-8019-2013, 2013.

753 Zhang, Q., Alfarra, M. R., Worsnop, D. R., Allan, J. D., Coe, H., Canagaratna, M. R. and Jimenez,
754 J. L.: Deconvolution and quantification of hydrocarbon-like and oxygenated organic aerosols based on
755 aerosol mass spectrometry, *Environ. Sci. Technol.*, 39, 4938-4952, doi:10.1021/es0485681, 2005.

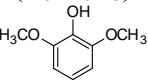
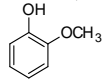
756 Zhang, Q., Jimenez, J., Canagaratna, M., Ulbrich, I., Ng, N., Worsnop, D. and Sun, Y.:
757 Understanding atmospheric organic aerosols via factor analysis of aerosol mass spectrometry: a review,
758 *Anal. Bioanal. Chem.*, 401, 3045-3067, doi:10.1007/s00216-011-5355-y, 2011.

759 Zhang, Q., Jimenez, J. L., Canagaratna, M. R., Allan, J. D., Coe, H., Ulbrich, I., Alfarra, M. R.,
760 Takami, A., Middlebrook, A. M., Sun, Y. L., Dzepina, K., Dunlea, E., Docherty, K., DeCarlo, P. F.,
761 Salcedo, D., Onasch, T., Jayne, J. T., Miyoshi, T., Shimojo, A., Hatakeyama, S., Takegawa, N., Kondo,
762 Y., Schneider, J., Drewnick, F., Borrmann, S., Weimer, S., Demerjian, K., Williams, P., Bower, K.,
763 Bahreini, R., Cottrell, L., Griffin, R. J., Rautiainen, J., Sun, J. Y., Zhang, Y. M. and Worsnop, D. R.:
764 Ubiquity and dominance of oxygenated species in organic aerosols in anthropogenically-influenced
765 Northern Hemisphere midlatitudes, *Geophys. Res. Lett.*, 34, L13801, doi:10.1029/2007GL029979, 2007.

766

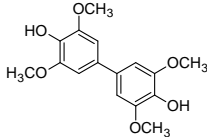
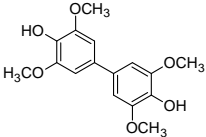
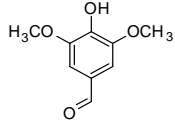
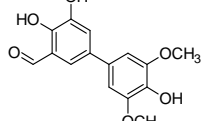
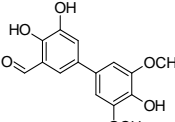
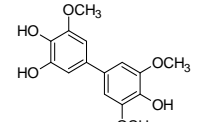
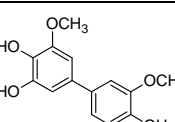
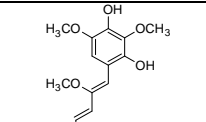
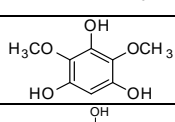
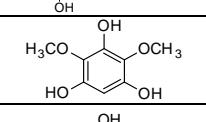
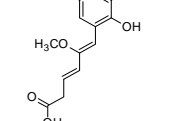
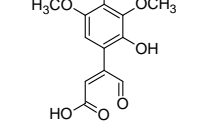
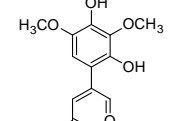
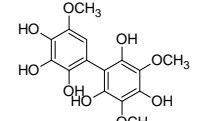
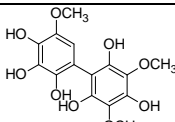
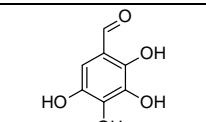
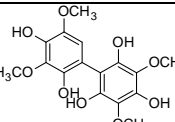
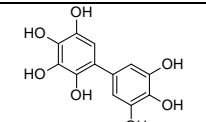
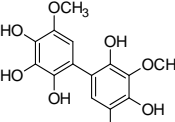
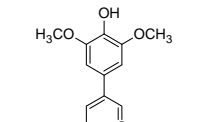
767 **Tables and Figures**768 **Table 1.** Summary of the chemical characteristics of phenolic aqSOA formed under different experimental conditions.

769

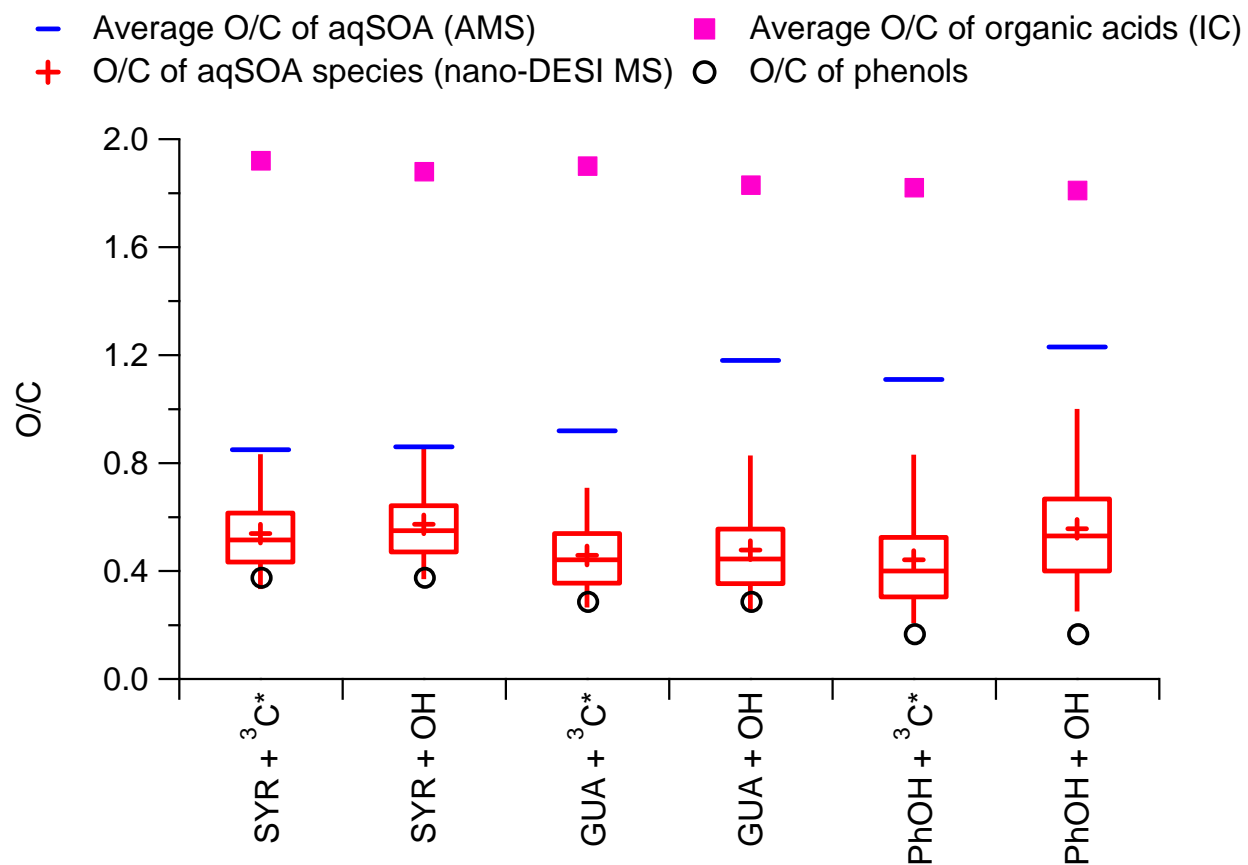
Sample information			AMS results						Nano-DESI MS results		IC results	TOC results
Precursor	Oxidant	$t_{1/2}^a$ (min)	OM/OC	O/C	H/C	OS _C ^b	$\Sigma m/z \geq 80^c$ (%)	Dimer ^d (%)	# of molecules ^e	# of common molecules	Organic acids (% of TOC) ^f	Dissolved volatile species ^g (%)
Syringol (C ₈ H ₁₀ O ₃) 	³ C*	16	2.29	0.85	1.66	0.04	13.3	-	1156	149	0.8	6.6
	•OH	45	2.27	0.86	1.64	0.08	12.3	-	998		0.7	5.9
Guaiacol (C ₇ H ₈ O ₂) 	³ C*	35	2.37	0.92	1.79	0.05	14.7	0.70	827		0.8	4.6
	•OH	160	2.72	1.18	1.85	0.51	9.8	0.15	871		2.2	2.7
Phenol (C ₆ H ₆ O) 	³ C*	480	2.63	1.11	1.70	0.52	8.8	0.51	721		2.1	2.8
	•OH	672	2.79	1.23	1.72	0.74	6.8	0.01	445		3.8	5.7

770 ^a $t_{1/2}$ is the time when approximately half of the phenolic precursor was reacted (as monitored by HPLC/UV-vis).771 ^b OS_C indicates the oxidation state of the carbon atom ($= 2 \times \text{O/C} - \text{H/C}$)772 ^c % of total ion signal at $m/z \geq 80$ in the AMS spectra.773 ^d estimated based on the signal contribution of the molecular ions of the dimers in the AMS spectra and the NIST spectra. NIST spectrum of syringol dimer is not available.774 ^e total number of molecules identified in the (+) ion mode and (-) ion mode nano-DESI MS spectra.775 ^f % of organic carbon mass in aqSOA accounted for by the sum of 8 organic acids (formate, acetate, pyruvate, malate, oxalate, malonate, fumarate, and mealeate).776 ^g dissolved volatile species is calculated as the differences in TOC between flash-frozen and blown-down samples after correction for the mass of unreacted precursors.

781 **Table 2.** Top 10 most abundant compounds in syringol SOA formed in $^3\text{C}^*$ - and $\bullet\text{OH}$ -mediated
 782 reactions identified with (-) nano-DESI MS.

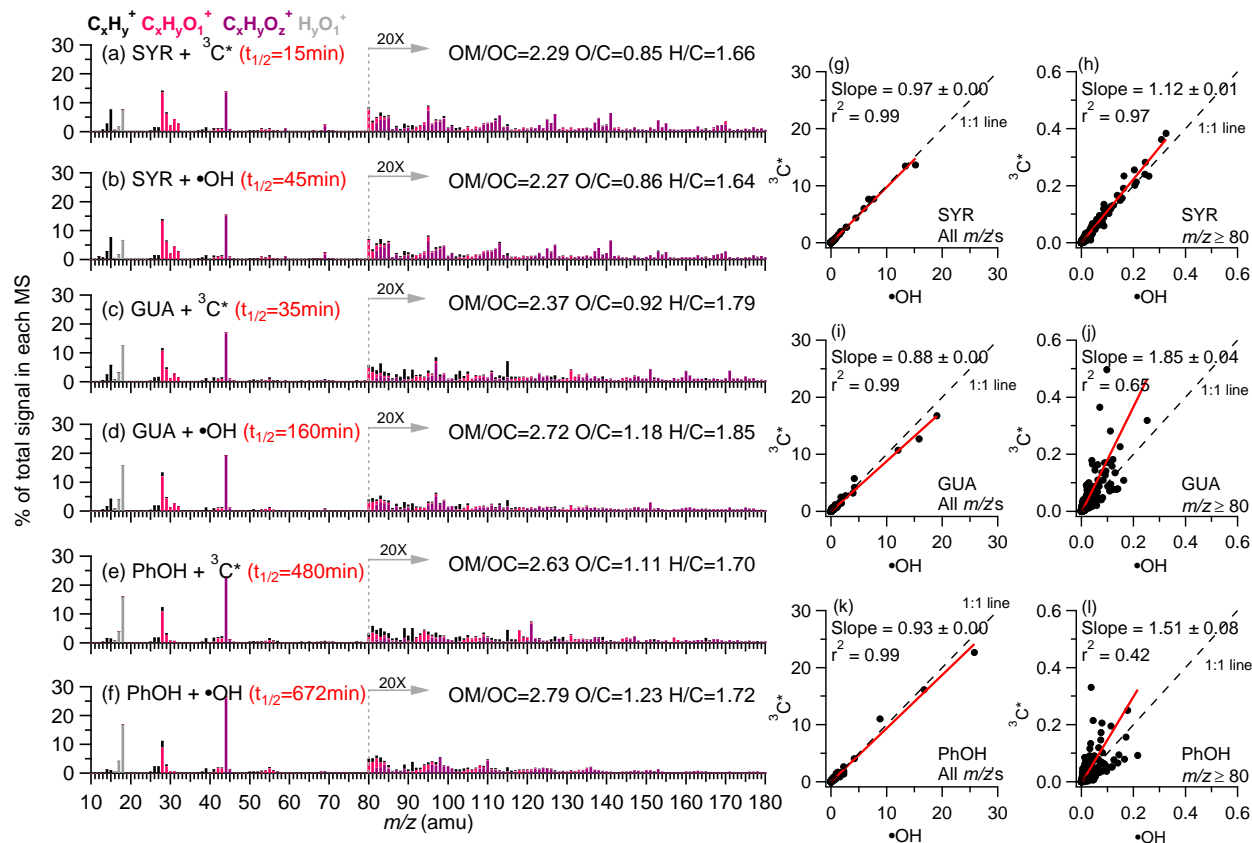
No.	$^3\text{C}^*$ reaction			$\bullet\text{OH}$ reaction		
	Molecular formula ^a	Proposed structure	DBE	Molecular formula ^a	Proposed structure	DBE
1	$\text{C}_{16}\text{H}_{18}\text{O}_6$ (306.1103)		8	$\text{C}_{16}\text{H}_{18}\text{O}_6$ (306.1103)		8
2	$\text{C}_9\text{H}_{10}\text{O}_4$ (182.0579)		5	$\text{C}_{15}\text{H}_{14}\text{O}_6$ (290.0790)		9
3	$\text{C}_{15}\text{H}_{14}\text{O}_6$ (290.0790)		9	$\text{C}_{15}\text{H}_{16}\text{O}_6$ (292.0946)		8
4	$\text{C}_{15}\text{H}_{16}\text{O}_6$ (292.0946)		8	$\text{C}_{15}\text{H}_{18}\text{O}_7$ (310.1052)		7
5	$\text{C}_8\text{H}_{10}\text{O}_5$ (186.0528)		4	$\text{C}_8\text{H}_{10}\text{O}_5$ (186.0528)		4
6	$\text{C}_{15}\text{H}_{18}\text{O}_7$ (310.1052)		7	$\text{C}_{12}\text{H}_{12}\text{O}_7$ (268.0583)		7
7	$\text{C}_{12}\text{H}_{12}\text{O}_7$ (268.0583)		7	$\text{C}_{15}\text{H}_{16}\text{O}_9$ (340.0794)		8
8	$\text{C}_{15}\text{H}_{16}\text{O}_9$ (340.0794)		8	$\text{C}_7\text{H}_6\text{O}_5$ (170.0215)		5
9	$\text{C}_{16}\text{H}_{18}\text{O}_9$ (354.0950)		8	$\text{C}_{12}\text{H}_{10}\text{O}_7$ (266.0426)		8
10	$\text{C}_{15}\text{H}_{14}\text{O}_8$ (322.0688)		9	$\text{C}_{12}\text{H}_{12}\text{O}_6$ (252.0634)		7

783
 784 ^a Molecular formula of top 10 most abundant compounds with their exact mass in the
 785 parenthesis.

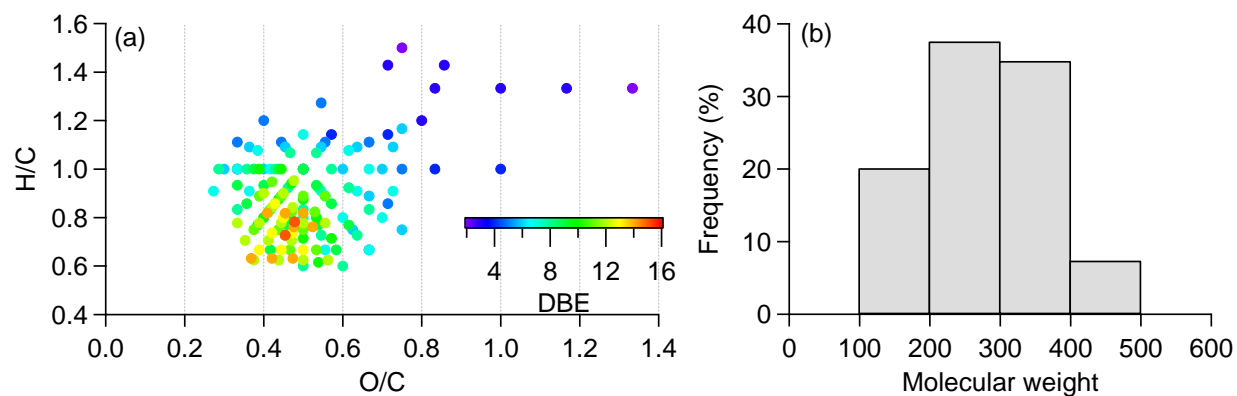


786

787 **Figure 1.** The average O/C ratios of aqSOA formed from the reactions of syringol
 788 (SYR), guaiacol (GUA), and phenol (PhOH) with $^3\text{C}^*$ and $\bullet\text{OH}$, respectively determined by
 789 AMS (blue bars) and the average O/C of organic acids determined by IC (pink squares). The
 790 distributions of the O/C of individual molecules in the aqSOA determined by nano-DESI MS are
 791 shown in box plots, in which the whiskers above and below the boxes indicate the 95th and 5th
 792 percentiles, the upper and lower boundaries of the boxes indicate the 75th and 25th percentiles,
 793 and the lines in the boxes indicate the median values and the cross symbols indicate the mean
 794 values. The O/C of the precursors are shown as black circles.



795
 796 **Figure 2.** AMS spectra of aqSOA formed from the reactions of (a-b) syringol (SYR), (c-
 797 d) guaiacol (GUA), and (e-f) phenol (PhOH) with $^{13}\text{C}^*$ and $\bullet\text{OH}$, respectively. The peaks are
 798 color-coded according to four ion categories: C_xH_y^+ , $\text{C}_x\text{H}_y\text{O}_1^+$, $\text{C}_x\text{H}_y\text{O}_z^+$, and H_yO_1^+ ($x \geq 1$; $y \geq 0$;
 799 $z \geq 2$). The ion signals at $m/z \geq 80$ are enhanced by a factor of 20 for clarity. The photoreaction
 800 time and the elemental ratios of the aqSOA are shown in the legends. Scatter plots that compare
 801 the mass spectra of aqSOA formed from two different oxidants for all m/z 's (g, i, k) and for m/z
 802 ≥ 80 (h, j, l) were performed using the orthogonal distance regression (ODR). The linear
 803 regression slopes and correlation coefficients are shown in the legends.

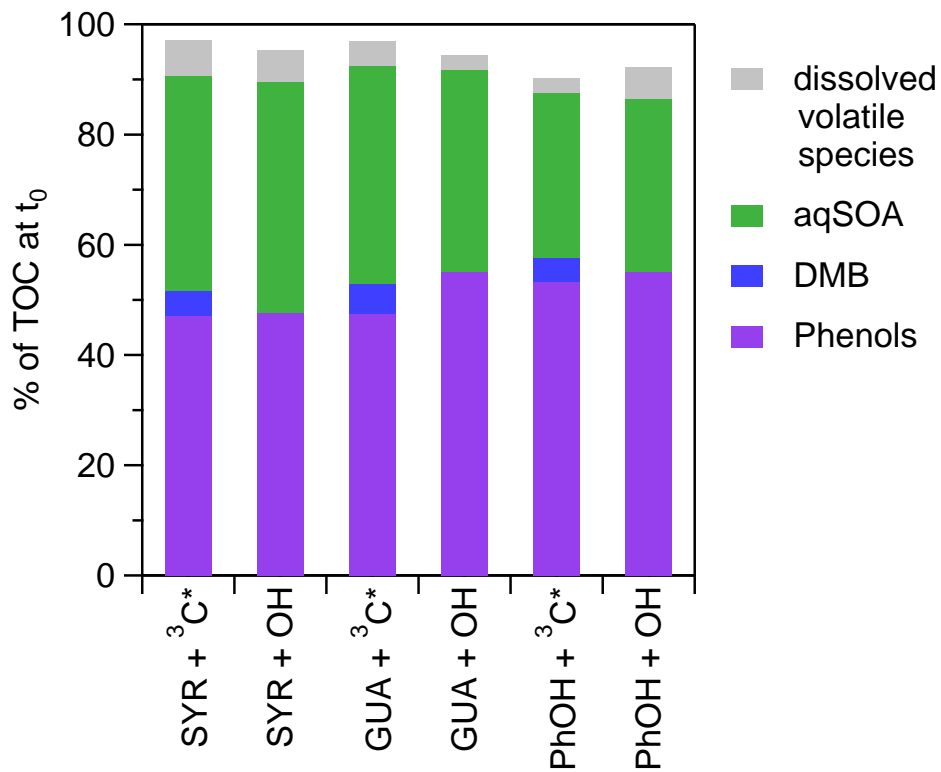


804

805 **Figure 3. (a)** Van Krevelen diagram of common molecules identified in every phenolic

806 aqSOA via nano-DESI MS analysis. Each data point is colored by its DBE value. **(b)** A

807 frequency histogram of the molecular weight of these common molecules.

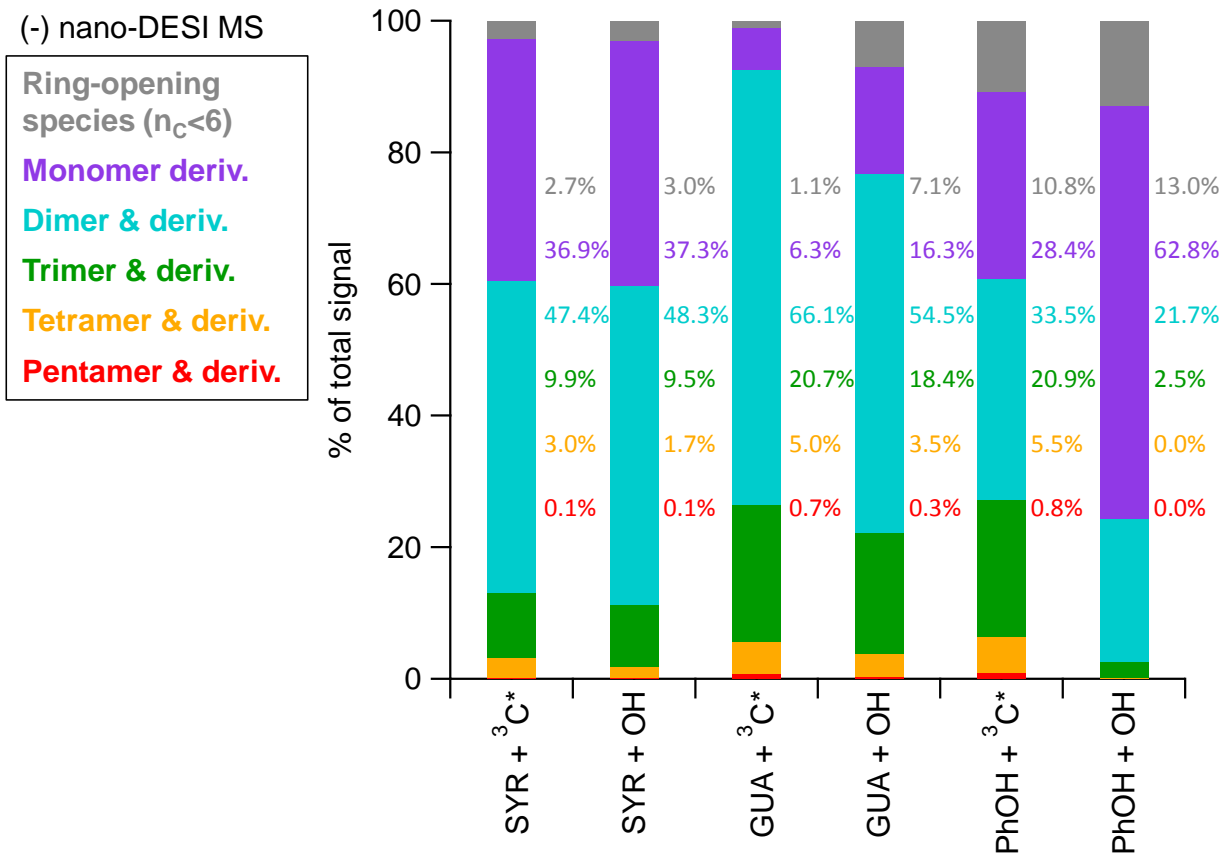


808

809 **Figure 4.** Contributions of reactants (phenolic precursor and DMB) and products

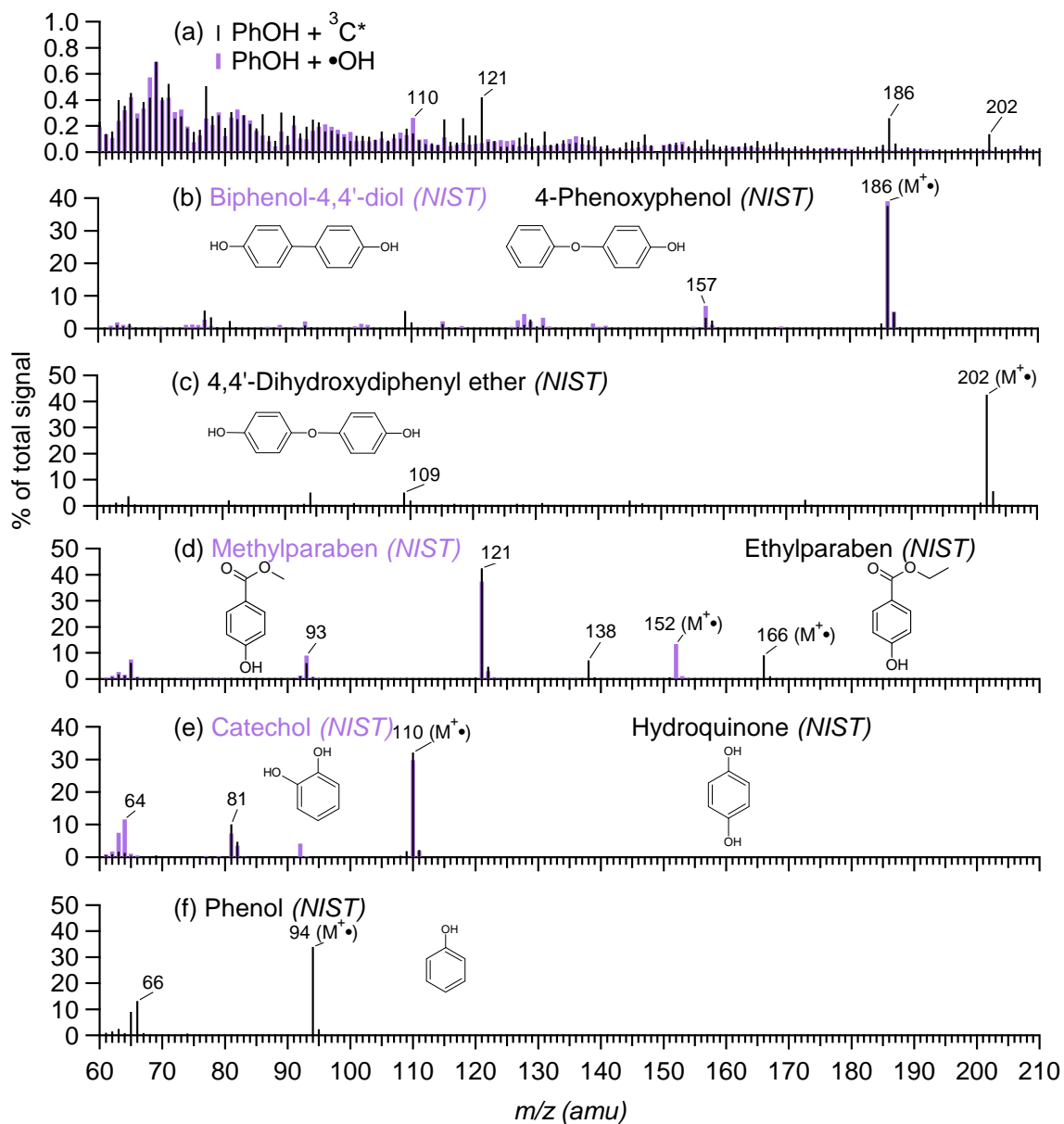
810 (dissolved volatile species and aqSOA) to the solution TOC after illumination to $t_{1/2}$. TOC

811 amounts are expressed relative to the TOC in the initial solution prior to illumination (i.e., at t_0).

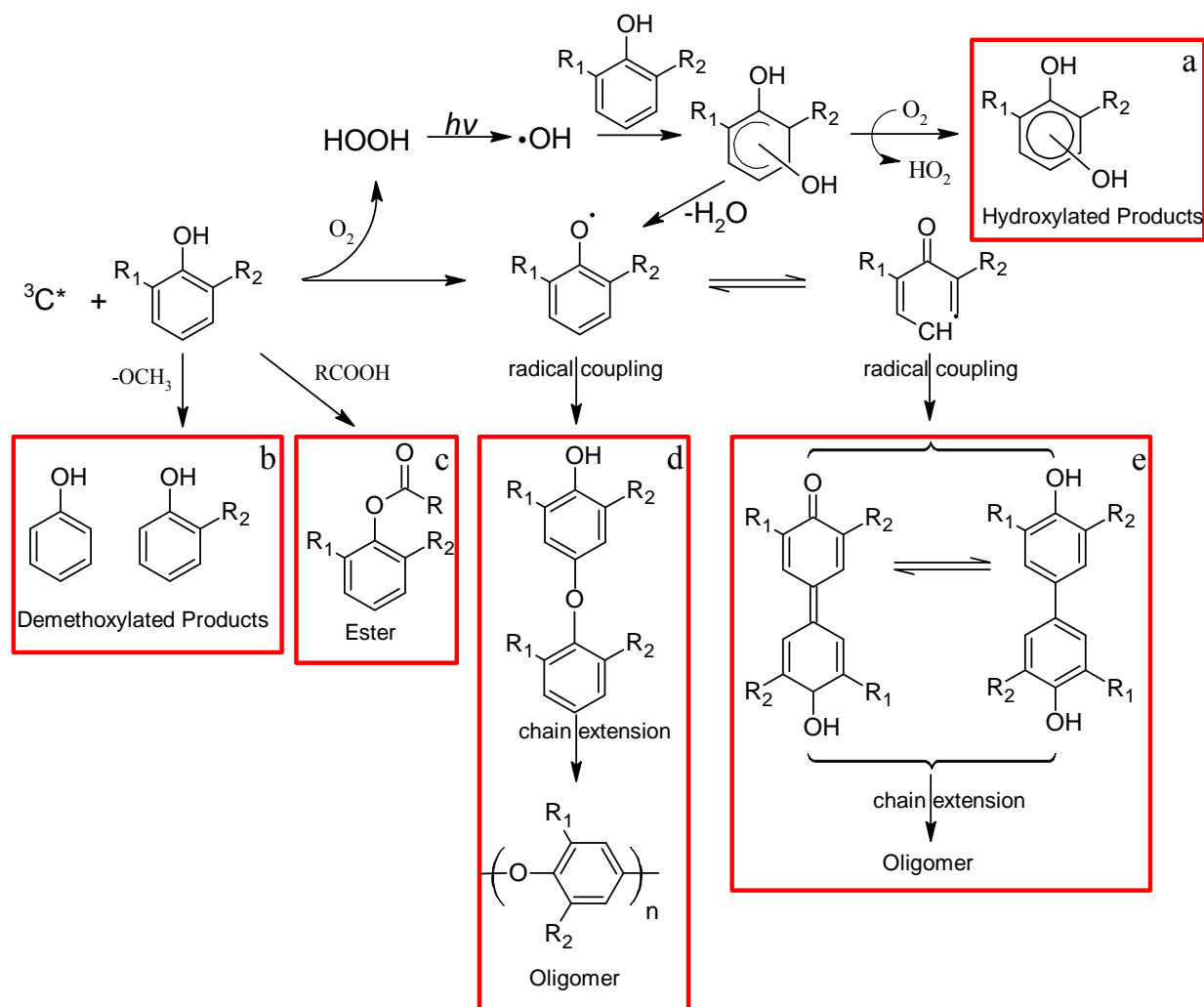


812

813 **Figure 5.** The signal weighted distributions of syringol (SYR), guaiacol (GUA) and
 814 phenol (PhOH) aqSOA formed in $^3C^*$ - and $\bullet OH$ -mediated reactions, respectively, based on the
 815 degree of oligomerization. The data are from the (-) nano-DESI MS spectra. Note that hexamer
 816 and derivatives are only found in (+) nano-DESI MS spectrum for GUA aqSOA initiated with
 817 $^3C^*$ and (-) nano-DESI MS spectrum for PhOH aqSOA initiated with $^3C^*$. The numbers indicate
 818 the contributions of individual categories to the total signals for each sample.



819
 820 **Figure 6.** Comparisons between (a) the AMS mass spectra (in integer m/z) of phenol
 821 (PhOH) aqSOA formed via reactions with $^3\text{C}^*$ and $\bullet\text{OH}$, respectively, and the NIST mass spectra
 822 of (b) biphenol-4,4'-diol and 4-phenoxyphenol, (c) 4,4'-dihydroxydiphenyl ether, (d)
 823 methylparaben and ethylparaben, (e) catechol and hydroquinone, and (f) phenol. The chemical
 824 structures for each compound are shown and the molecular ions ($\text{M}^{\bullet+}$) are marked.



825

826 **Figure 7.** A schematic illustrates the formation of hydroxylated species, dimers and

827 higher oligomers, esters, and demethoxylated products from aqueous photooxidation of phenolic

828 compounds. Species produced via pathways **a - e** may undergo further ring-opening processes to

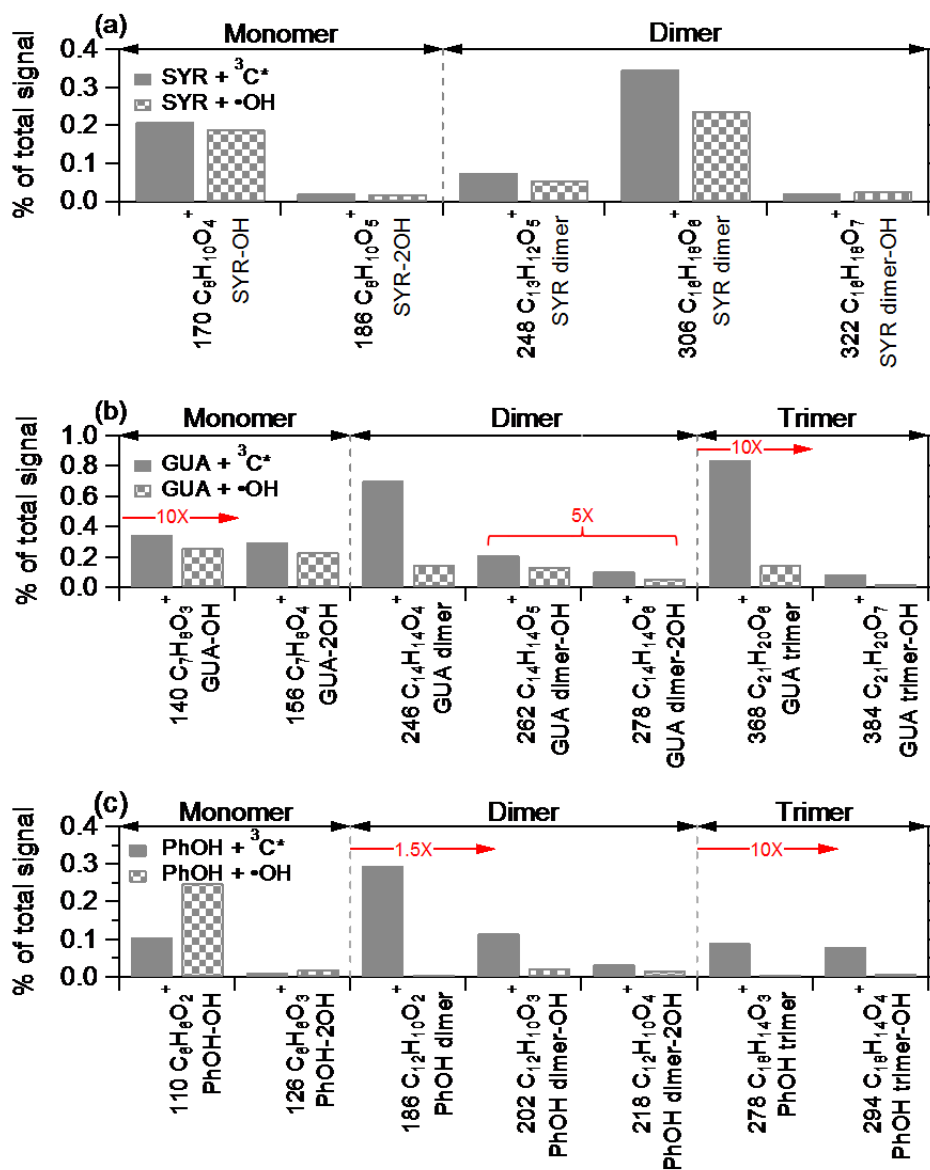
829 form ketones and carboxylic acids. Phenol: $\text{R}_1=\text{H}$, $\text{R}_2=\text{H}$; Guaiacol: $\text{R}_1=\text{OCH}_3$, $\text{R}_2=\text{H}$; Syringol:

830 $\text{R}_1=\text{OCH}_3$, $\text{R}_2=\text{OCH}_3$. Note that while radical coupling here is shown through the carbon

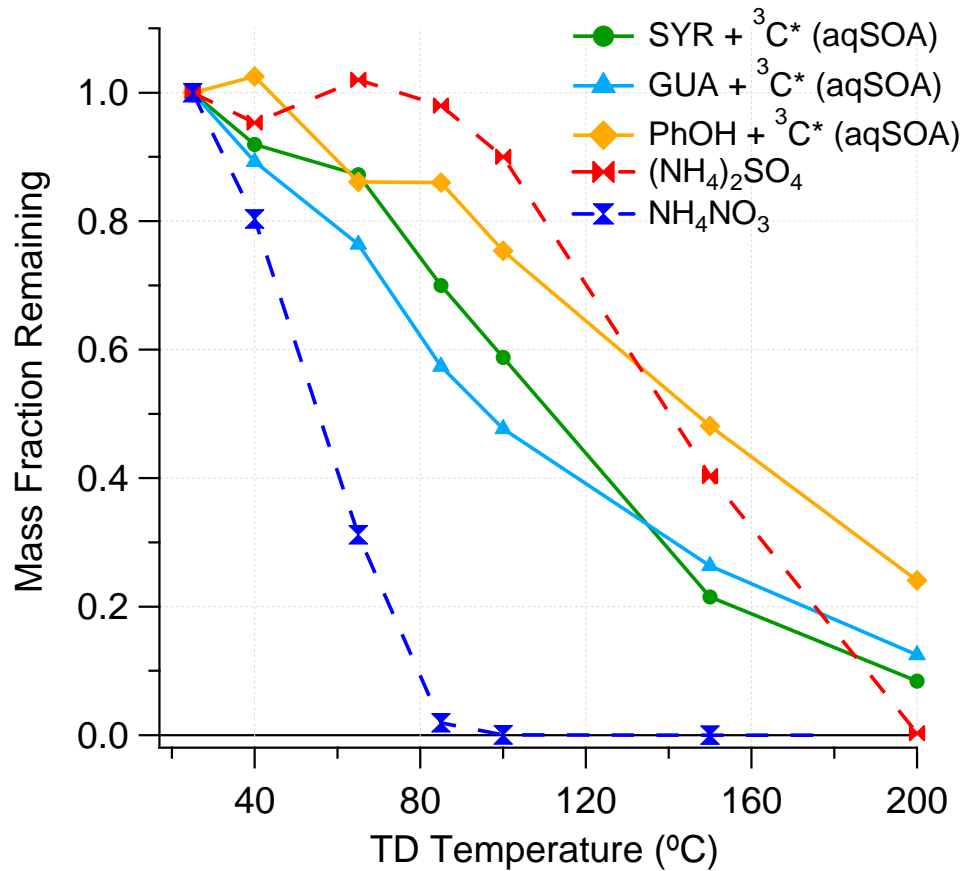
831 opposite (para) the phenoxy group, other geometric isomers will also be formed during these

832 reactions.

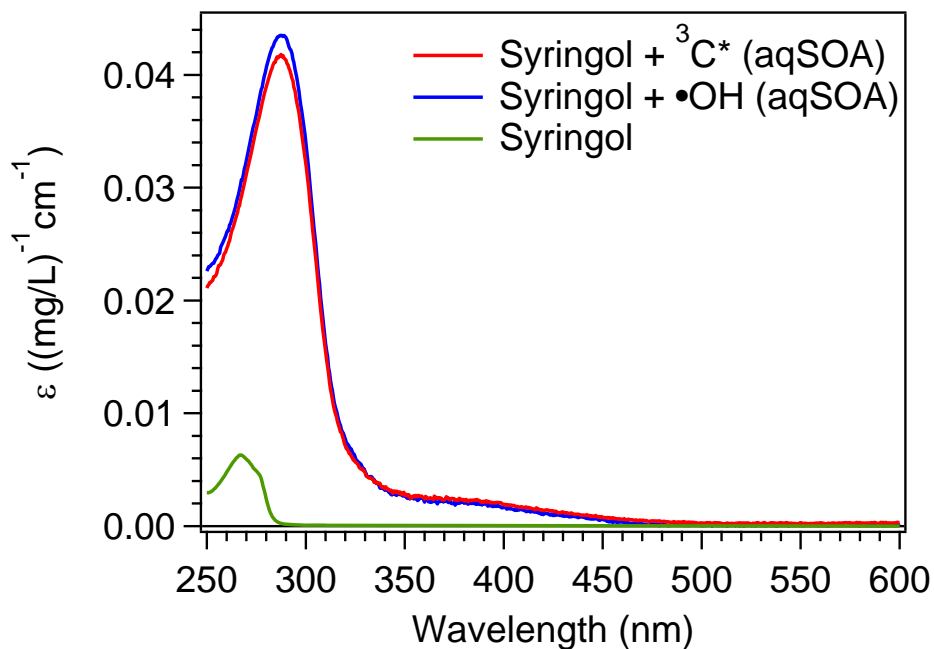
833



834
 835 **Figure 8.** Comparisons of the relative abundances of signature ions in the AMS spectra
 836 of the aqSOA of (a) syringol (SYR), (b) guaiacol (GUA), and (c) phenol (PhOH) produced from
 837 $^3\text{C}^*$ - and $\bullet\text{OH}$ -mediated reactions. The signal contributions of certain signature ions are
 838 enhanced for clarity. The m/z values of the signature ions are shown in front of the ion formula in
 839 the x-axes. Identities of possible parent compounds are shown to the right. 2OH represents 2
 840 additional hydroxyl groups attached to the aromatic ring.



841
 842 **Figure 9.** Mass thermograms of ammonium sulfate ((NH₄)₂SO₄), ammonium nitrate
 843 (NH₄NO₃), syringol (SYR), guaiacol (GUA) and phenol (PhOH) aqSOA formed in ³C*-
 844 mediated aqueous-phase reactions.



845

846 **Figure 10.** UV-vis spectra of syringol and syringol aqSOA formed in $^3\text{C}^*$ - and $\bullet\text{OH}$ -
847 mediated aqueous-phase reactions. The aqSOA spectra were corrected for absorbance
848 contributions from unreacted reactants (syringol and DMB).